

1 **Large but decreasing effect of ozone on the European carbon**
2 **sink**

3 Rebecca J Oliver¹, Lina M Mercado^{1,2}, Stephen Sitch², David Simpson^{3,4}, Belinda E Medlyn⁵,
4 Yan-Shih Lin⁵, Gerd A Folberth⁶

5

6 ¹ Centre for Ecology and Hydrology, Benson Lane, Wallingford, OX10 8BB, UK

7 ² College of Life and Environmental Sciences, University of Exeter, EX4 4RJ, Exeter, UK

8 ³ EMEP MSC-W Norwegian Meteorological Institute, PB 43, NO-0313, Oslo, Norway

9 ⁴ Dept. Space, Earth & Environment, Chalmers University of Technology, Gothenburg, SE-41296 Sweden

10 ⁵ Hawkesbury Institute for the Environment, Western Sydney University, Locked Bag 1797, Penrith NSW 2751
11 Australia

12 ⁶ Met Office Hadley Centre, Exeter, UK.

13 *Correspondence to:* Rebecca Oliver (rfu@ceh.ac.uk)

14

15

16

17

18

19

20

21

22

23

24

25

26 **Abstract**

27

28 The capacity of the terrestrial biosphere to sequester carbon and mitigate climate change is governed by the ability
29 of vegetation to remove emissions of CO₂ through photosynthesis. Tropospheric O₃, a globally abundant and
30 potent greenhouse gas, is, however, known to damage plants, causing reductions in primary productivity, yet the
31 impact of this gas on European vegetation and the land carbon sink is largely unknown. Despite emission control
32 policies across Europe, background concentrations of tropospheric O₃ have risen significantly over the last
33 decades due to hemispheric-scale increases in O₃ and its precursors. Therefore, plants are exposed to increasing
34 background concentrations, at levels currently causing chronic damage. We use the JULES land-surface model
35 recalibrated for O₃ impacts on European vegetation, with an improved stomatal conductance parameterization, to
36 quantify the impact of tropospheric O₃, and its interaction with CO₂, on gross primary productivity (GPP) and
37 land carbon storage across Europe. A factorial set of model experiments showed that tropospheric O₃ can suppress
38 terrestrial carbon uptake across Europe over the period 1901 to 2050. By 2050, simulated GPP was reduced by 4
39 to 9% due to plant ozone damage and land carbon storage by 3 to 7%. The combined physiological effects of
40 elevated future CO₂ (acting to reduce stomatal opening) and reductions in O₃ concentrations resulted in reduced
41 O₃ damage in the future, contrary to predictions from earlier studies. This alleviation of O₃ damage by CO₂ induced
42 stomatal closure was around 1 to 2% for low and high sensitivity respectively (on both land carbon and GPP).
43 Reduced land carbon storage resulted from diminished soil carbon stocks consistent with the reduction in GPP.
44 Regional variations are identified with larger impacts shown for temperate Europe (GPP reduced by 10 to 20%)
45 compared to boreal regions (GPP reduced by 2 to 8%). These results highlight that O₃ damage needs to be
46 considered when predicting GPP and land carbon, and that the effects of O₃ on plant physiology need to be
47 considered in regional land carbon cycle assessments..

48

49

50

51

52

53

54

55

56

57

58 1 Introduction

59

60 The terrestrial biosphere absorbs around 30% of anthropogenic CO₂ emissions and acts to mitigate climate change
61 (Le Quéré et al., 2015). Early estimates of the European carbon balance suggest a terrestrial carbon sink of between
62 135 to 205 TgC yr⁻¹ (Janssens et al., 2003). Schulze et al. (2009) determined a larger carbon sink of 274 TgC yr⁻¹,
63 and more recent estimates suggest a European terrestrial sink of between 146 to 184 TgC yr⁻¹ (Luysaert et al.,
64 2012). The carbon sink capacity of land ecosystems is dominated by the ability of vegetation to sequester carbon
65 through photosynthesis and release it back to the atmosphere through respiration. Therefore, any change in the
66 balance of these fluxes will alter ecosystem source-sink behaviour.

67

68 In recent decades much attention has focussed on the effects of rising atmospheric CO₂ on vegetation productivity
69 (Ceulemans and Mousseau, 1994;Norby et al., 2005;Norby et al., 1999;Saxe et al., 1998). The Norby et al. (2005)
70 synthesis of Free Air CO₂ Enrichment (FACE) experiments suggests a median stimulation ($23 \pm 2\%$) of forest
71 NPP in response to a doubling of CO₂. Similar average increases (20%) were observed for C₃ crops, although this
72 translated into smaller gains in biomass (17%) and crop yields (13%) (Long et al., 2006). Little attention, however,
73 has been given to tropospheric ozone (O₃), a globally abundant air pollutant recognised as one of the most
74 damaging pollutants for forests (Karlsson et al., 2007;Royal-Society, 2008;Simpson et al., 2014b). Tropospheric
75 O₃ is a secondary air pollutant formed by photochemical reactions involving carbon monoxide (CO), volatile
76 organic compounds (VOCs), methane (CH₄) and nitrogen oxides (NO_x) from both man-made and natural sources,
77 as well as downward transport from the stratosphere and lightning which is a source of NO_x. The phytotoxic
78 effects of O₃ exposure are shown to decrease vegetation productivity and biomass, with consequences for
79 terrestrial carbon sequestration (Felzer et al., 2004;Loya et al., 2003;Mills et al., 2011b;Sitch et al., 2007). Few
80 studies, however, consider the simultaneous effects of exposure to both gases, and few Earth-system models
81 (ESMs) currently explicitly consider the role of tropospheric O₃ in terrestrial carbon dynamics (IPCC, 2013), both
82 of which are key to understanding the carbon sequestration potential of the land-surface, and future carbon
83 dynamics regionally and globally.

84

85 Due to increased anthropogenic precursor emissions over the industrial period, background concentrations of
86 ground-level O₃ have risen (Vingarzan, 2004). O₃ levels at the start of the 20th century are estimated to be around
87 10 ppb for the site Montsouris Observatory near Paris, data for Arkona on the Baltic coast increased from ca. 15
88 ppb in the 1950s to 20-27 ppb by the early 1980s, and the Irish coast site Mace Head shows around 40 ppb by the
89 year 2000 (Logan et al., 2012;Parrish et al., 2012). Present day annual average background O₃ concentrations
90 reported in the review of (Vingarzan, 2004) show O₃ concentrations range between approximately 20 and 45ppb,
91 with the greatest increase occurring since the 1950s. Trends vary from site to site though, even on a decadal basis
92 (Logan et al., 2012;Simpson et al., 2014b), depending, for example, on local/regional trends in precursor
93 (especially NO_x) emissions, elevation, and exposure to long-range transport. Nevertheless, there is some
94 indication that background O₃ levels over the mid-latitudes of the Northern Hemisphere have continued to rise at
95 a rate of approximately 0.5–2% per year, although not uniform (Vingarzan, 2004). As a result of controls on
96 precursor emissions in Europe and North America, peak O₃ concentrations in these regions have decreased or
97 stabilised over recent decades (Cooper et al., 2014;Logan et al., 2012;Parrish et al., 2012;Simpson et al., 2014b).

98 Nevertheless, climate change may increase the frequency of weather events conducive to peak O₃ incidents in the
99 future (e.g. summer droughts and heat-waves; e.g., (Sicard et al., 2013), and may increase biogenic emissions of
100 the O₃-precursors isoprene and NO_x, although such impacts are subject to great uncertainty (Simpson et al.,
101 2014b;Young et al., 2013;Young et al., 2009). Intercontinental transport of air pollution from regions such as Asia
102 that currently have poor emission controls are thought to contribute substantially to rising background O₃
103 concentrations over the last decades (Cooper et al., 2010;Verstraeten et al., 2015). Northern Hemisphere
104 background concentrations of O₃ are now close to established levels for impacts on human health and the terrestrial
105 environment (Royal-Society, 2008). Therefore, although peak O₃ concentrations are in decline across Europe,
106 plants are exposed to increasing background levels, at levels currently causing chronic damage (Mills et al.,
107 2011b). Intercontinental transport means future O₃ concentrations in Europe are dependent on how O₃ precursor
108 emissions evolve globally.

109

110 Elevated O₃ concentrations impact agricultural yields and nutritional quality of major crops (Ainsworth et al.,
111 2012;Avnery et al., 2011), with consequences for global food security (Tai et al., 2014). As well as being a
112 significant air pollutant, O₃ is a potent greenhouse gas (Royal-Society, 2008). High levels of O₃ are damaging to
113 ecosystem health and reduce the global land carbon sink (Arneth et al., 2010;Sitch et al., 2007). Reduced uptake
114 of carbon by plant photosynthesis due to O₃ damage allows more CO₂ to remain in the atmosphere. This effect of
115 O₃ on plant physiology represents an additional climate warming to the direct radiative forcing of O₃ (Collins et
116 al., 2010;Sitch et al., 2007), the magnitude of which, however, remains highly uncertain (IPCC, 2013).

117

118 Dry deposition of O₃ to terrestrial surfaces, primarily uptake by stomata on plant foliage and deposition on external
119 surfaces of vegetation, is a large sink for ground level O₃ (Fowler et al., 2009;Fowler et al., 2001). On entry to
120 sub-stomatal spaces, O₃ reacts with other molecules to form reactive oxygen species (ROS). Plants can tolerate a
121 certain level of O₃ depending on their capacity to scavenge and detoxify the ROS (Ainsworth et al., 2012). Above
122 this critical level, long-term chronic O₃ exposure reduces plant photosynthesis and biomass accumulation
123 (Ainsworth, 2008;Ainsworth et al., 2012;Matyssek et al., 2010a;Wittig et al., 2007;Wittig et al., 2009), either
124 directly through effects on photosynthetic machinery such as reduced Rubisco content (Ainsworth et al.,
125 2012;Wittig et al., 2009) and/or indirectly by reduced stomatal conductance (g_s) (Kitao et al., 2009;Wittig et al.,
126 2007), alters carbon allocation to different pools (Grantz et al., 2006;Wittig et al., 2009), accelerates leaf
127 senescence (Ainsworth, 2008;Nunn et al., 2005;Wittig et al., 2009) and changes plant susceptibility to biotic stress
128 factors (Karnosky et al., 2002;Percy et al., 2002).

129

130 The response of plants to O₃ is very wide ranging as reported in the literature from different field studies. The
131 Wittig et al. (2007) meta-analysis of temperate and boreal tree species showed future concentrations of O₃
132 predicted for 2050 significantly reduced leaf level light saturated net photosynthetic uptake (-19%, range: -3% to
133 -28%) and g_s (-10%, range: +5% to -23%) in both broadleaf and needle leaf tree species. In the Feng et al. (2008)
134 meta-analysis of wheat, projected O₃ concentrations for the future reduced aboveground biomass (-18%)
135 photosynthetic rate (-20%) and g_s (-22%). One of few long-term field based O₃ exposure studies (AspenFACE)
136 showed that after 11 years of exposing mature trees to elevated O₃ concentrations, O₃ decreased ecosystem carbon
137 content (-9%), and decreased NPP (-10%), although the O₃ effect decreased through time (Talhelm et al., 2014).

138 Zak et al. (2011) showed this was partly due to a shift in community structure as O₃-tolerant species, competitively
139 inferior in low O₃ environments, out competed O₃-sensitive species. GPP was reduced (-12% to -19%) at two
140 Mediterranean ecosystems exposed to elevated O₃ studied by Fares et al. (2013). Biomass of mature beech trees
141 was reduced (-44%) after 8 years of exposure to elevated O₃ (Matyssek et al., 2010a). After 5 years of O₃ exposure
142 in a semi-natural grassland, annual biomass production was reduced (-23%), and in a Mediterranean annual
143 pasture O₃ exposure significantly reduced total aboveground biomass (up to -25%) (Calvete-Sogo et al., 2014).
144 However, these were empirical studies at individual sites, and these focus on O₃ effects on plant physiology and
145 productivity, but do not quantify the impact on the land carbon sink. Modelling studies are needed to scale site
146 observations to the regional and global scales. Models generally suggest that plant productivity and carbon
147 sequestration will decrease with O₃ pollution, though the magnitudes vary. For example, based on a limited dataset
148 to parameterise plant O₃ damage for a global set of plant functional types, Sitch et al. (2007) predicted a decline
149 in global GPP of 14 to 23% by 2100. A second study by Lombardozzi et al. (2015) similarly predicted a 10.8%
150 decrease of global GPP. Here we take a regional approach and take advantage of new measurements specifically
151 for European vegetation and conduct a dedicated analysis for the European region.

152

153 Understanding the response of plants to elevated tropospheric O₃ is challenged by the large variation in O₃
154 sensitivity both within and between species (Karnosky et al., 2007; Kubiske et al., 2007; Wittig et al., 2009).
155 Additionally, other environmental stresses that affect stomatal behaviour will affect the rate of O₃ uptake and
156 therefore the response to O₃ exposure, such as high temperature, drought and changing concentrations of
157 atmospheric CO₂ (Mills et al., 2016; Fagnano et al., 2009; Kitao et al., 2009; Löw et al., 2006), such that the
158 response of vegetation to O₃ is a balance between opposing drivers of stomatal behaviour. Increasing
159 concentrations of atmospheric CO₂, for example, are suggested to provide some protection against O₃ damage by
160 causing stomata to close (Harmens et al., 2007; Wittig et al., 2007), however the long-term effects of CO₂
161 fertilisation on plant growth and carbon storage remain uncertain (Baig et al., 2015; Ciais et al., 2013). Further, in
162 some studies, stomata have been shown to respond sluggishly, losing their responsiveness to environmental
163 stimuli with exposure to O₃ which can lead to higher O₃ uptake, increased water-loss and therefore greater
164 vulnerability to environmental stresses such as drought (Mills et al., 2016; Mills et al., 2009; Paoletti and Grulke,
165 2010; Wilkinson and Davies, 2009).

166

167 Given the critical role g_s plays in the uptake of both CO₂ and O₃, we use an alternative representation and
168 parameterisation of g_s in JULES by implementing the Medlyn *et al.* (2011) g_s formulation. This model is based
169 on the optimal theory of stomatal behaviour, it does not currently include a representation of sluggish stomatal
170 control, but it has the following advantages over the current JULES g_s formulation of Jacobs (1994): i) a single
171 parameter (g_1) which represents the marginal cost of water-use, compared to two parameters in Jacobs (1994)
172 representing the critical humidity deficit at the leaf surface (d_{crit}) and the ci/ca ratio at the leaf critical
173 humidity deficit (f_l) (Clark et al., 2011); ii) easier to parameterise with leaf or canopy level observations of
174 photosynthesis, g_s and humidity – all variables that are commonly measured, and (iii) values of g_1 are available
175 for many different plant functional types (PFTs) derived from a global data set of leaf-level measurements (Lin et
176 al., 2015).

177

178 The main objective of this work is to assess the impact of historical and projected (1901 to 2050) changes in
179 tropospheric O₃ and atmospheric CO₂ concentration on predicted GPP and the land-carbon sink for Europe.
180 These are the two greenhouse gases that directly affect plant photosynthesis and g_s . We use a factorial suite of
181 model experiments, using the Joint UK land environment simulator (JULES) (Best et al., 2011; Clark et al.,
182 2011), the land-surface model of the UK Earth System Model (UKESM) (Collins et al., 2011) to simulate plant
183 O₃ uptake and damage, and to look at the interaction between O₃ and CO₂. In this work, plant O₃ damage in
184 JULES is developed further by introducing a term for dry deposition of O₃ to external plant surfaces, an
185 important sink for tropospheric O₃ that was previously absent from the model. Further, the model is re-
186 calibrated using the latest observations of vegetation sensitivity to O₃, with the addition of a separate
187 parameterisation for temperate/boreal regions versus the Mediterranean. The plant O₃ sensitivity of each PFT in
188 JULES was re-calibrated for both a high and low plant O₃ sensitivity to account for the large variation in O₃
189 sensitivity within and between species. This includes separate sensitivities for Mediterranean regions, and for
190 agricultural crops (wheat) versus natural grassland. We make a separate distinction for the Mediterranean region
191 where possible because the work of Büker et al. (2015) showed that different O₃ dose-response relationships are
192 needed to describe the O₃ sensitivity of dominant Mediterranean trees. In addition, we introduce an alternative g_s
193 scheme into JULES as described above. JULES is forced with spatially varying hourly O₃ concentrations from a
194 high resolution atmospheric chemistry model for Europe, therefore our simulations account for diurnal
195 variations in O₃ concentration and O₃ responses allowing for more accurate estimations of O₃ uptake by
196 vegetation. We do not attempt to make a full assessment of the carbon cycle of Europe, instead we target O₃
197 damage, and its interaction with CO₂, which is currently a missing component in earlier carbon cycle
198 assessments (Le Quéré et al., 2017; Sitch et al., 2015). To this end, we prescribe changing O₃ and CO₂
199 concentrations from 1901 to 2050, but use a fixed pre-industrial climate. We acknowledge the use of a 'fixed'
200 pre-industrial climate omits the additional uncertainty of the interaction between climate change and g_s which
201 will affect the rate of O₃ uptake and therefore O₃ concentrations. To understand the impact of these complex
202 feedback mechanisms is an important area for future work, but in the current study our aim is to isolate the
203 physiological response of plants to both O₃ and CO₂, and determine the sensitivity of predicted GPP and the
204 land carbon sink to this process, as the impact of O₃ on European vegetation and the land carbon sink currently
205 remains largely unknown.

206

207

208

209 **2 Methods**

210

211 **2.1 Representation of O₃ effects in JULES**

212

213 JULES calculates the land-atmosphere exchanges of heat, energy, mass, momentum and carbon on a sub-daily
214 time step, and includes a dynamic vegetation model (Best et al., 2011; Clark et al., 2011; Cox, 2001). This work
215 uses JULES version 3.3 (<http://www.jehmr.org>) at 0.5° x 0.5° spatial resolution and hourly model time step, the
216 spatial domain is shown in Fig. S5. JULES has a multi-layer canopy radiation interception and photosynthesis
217 scheme (10 layers in this instance) that accounts for direct and diffuse radiation, sun fleck penetration through the

218 canopy, inhibition of leaf respiration in the light and change in photosynthetic capacity with depth into the canopy
 219 (Clark et al., 2011; Mercado et al., 2009). Soil water content also affects the rate of photosynthesis and g_s . It is
 220 modelled using a dimensionless soil water stress factor, β , which is related to the mean soil water concentration
 221 in the root zone, and the soil water contents at the critical and wilting point (Best *et al.*, 2011).

222

223 To simulate the effects of O_3 deposition on vegetation productivity and water use, JULES uses the flux-gradient
 224 approach of Sitch *et al.*, (2007), modified to include non-stomatal deposition following Tuovinen et al. (2009).
 225 JULES uses a coupled model of g_s and photosynthesis; because of the relationship between these two fluxes, the
 226 direct effect of O_3 damage on photosynthetic rate also leads to a reduction in g_s . Changes in atmospheric CO_2
 227 concentration also affect photosynthetic rate and g_s , consequently the interaction between changing concentrations
 228 of both gases is allowed for. Specifically, the potential net photosynthetic rate (A_p , mol CO_2 m^{-2} s^{-1}) is modified
 229 by an 'O₃ uptake' factor (F , the fractional reduction in photosynthesis), so that the actual net photosynthesis (A_{net} ,
 230 mol CO_2 m^{-2} s^{-1}) is given by equation 1 (Clark *et al.*, 2011, Sitch *et al.*, 2007).

231

$$232 \quad A_{net} = A_p F \quad (1)$$

233

234 The O_3 uptake factor (F) is defined as:

235

$$236 \quad F = 1 - a * \max[F_{O_3} - F_{O_3crit}, 0.0] \quad (2)$$

237

238 F_{O_3} is the instantaneous leaf uptake of O_3 (nmol m^{-2} s^{-1}), F_{O_3crit} is a PFT-specific threshold for O_3 damage (nmol
 239 m^{-2} PLA s^{-1} , projected leaf area), and 'a' is a PFT-specific parameter representing the fractional reduction of
 240 photosynthesis with O_3 uptake by leaves. Following Tuovinen et al. (2009), the flux of O_3 through stomata, F_{O_3} ,
 241 is represented as follows:

242

$$243 \quad F_{O_3} = O_3 \left(\frac{g_b \left(\frac{g_l}{K_{O_3}} \right)}{g_b + \left(\frac{g_l}{K_{O_3}} \right) + g_{ext}} \right) \quad (3a)$$

244

245 O_3 is the molar concentration of O_3 at reference (canopy) level (nmol m^{-3}), g_b is the leaf-scale boundary layer
 246 conductance (m s^{-1} , eq 3b), g_l is the leaf conductance for water (m s^{-1}), K_{O_3} accounts for the different diffusivity of
 247 ozone to water vapour and takes a value of 1.51 after Massman (1998), and g_{ext} is the leaf-scale non-stomatal
 248 deposition to external plant surfaces (m s^{-1}) which takes a constant value of 0.0004 m s^{-1} after Tuovinen et al.
 249 (2009). The leaf-level boundary layer conductance (g_b) is calculated as in Tuovinen *et al.* (2009)

250

$$251 \quad g_b = \alpha L d^{-1/2} U^{-1/2} \quad (3b)$$

252

253 α is a constant (0.0051 m $s^{-1/2}$), Ld is the cross-wind leaf dimension (m) and U is wind speed at canopy height (m
 254 s^{-1}). The rate of O_3 uptake is dependent on g_s , which is dependent on photosynthetic rate. Given g_s is a linear
 255 function of photosynthetic rate in JULES (Clark et al., 2011), from eq 1 it follows that:

256

257 $g_s = g_l F$ (4)

258

259 The O₃ flux to stomata, F_{O_3} , is calculated at leaf level and then scaled to each canopy layer differentiating sunlit
 260 and shaded leaf photosynthesis, and finally summed up to the canopy level. Because the photosynthetic capacity,
 261 photosynthesis and therefore g_s decline with depth into the canopy, this in turn affects O₃ uptake, with the top leaf
 262 level contributing most to the total O₃ flux and the lowest level contributing least.

263

264 **2.2 Calibration of O₃ uptake model**

265

266 Here we use the latest literature on O₃ dose-response relationships derived from observed field data across Europe
 267 (CLRTAP, 2017) to determine the key PFT-specific O₃ sensitivity parameters in JULES (a and F_{O_3crit}). Each
 268 JULES PFT (broadleaf, needle leaf, C₃ and C₄ herbaceous, and shrub) was calibrated for a high and low plant O₃
 269 sensitivity to account for uncertainty in variation of species sensitivity to O₃, using the approach of Sitch *et al.*,
 270 (2007). For the C₃ herbaceous PFT – the dominant land cover type across Europe in this study (Fig. S1) - the O₃
 271 sensitivity was calibrated against observations for wheat to give a representation of agricultural regions (high plant
 272 O₃ sensitivity), versus natural grassland (low plant O₃ sensitivity), with a separate function for Mediterranean
 273 grasslands (low plant O₃ sensitivity) (Table S1 and Figure S2). Broadleaf tree and shrub PFTs were calibrated
 274 against the birch/beech observed O₃ dose-response functions for the high plant O₃ sensitivity, with a separate
 275 function for Mediterranean broadleaf trees (deciduous oaks), needle leaf trees were calibrated against the function
 276 for Norway spruce, all data for dose-response functions were from CLRTAP (2017). The low plant O₃ sensitivity
 277 functions for trees/shrubs were calibrated as being 20% less sensitive based on the difference in sensitivity
 278 between high and low sensitive tree species in the Karlsson *et al.* (2007) study. Due to limitations in data
 279 availability, the parameterisation for C₄ herbaceous uses the observed dose-responses for C₃ herbaceous, however
 280 the fractional cover of C₄ herbs across Europe is low (Fig. S1), so this assumption affects a very small percentage
 281 of land cover.

282

283 To calibrate each JULES PFT for sensitivity to O₃, JULES was run, varying the value of parameter a , until model
 284 output of change in NPP with cumulative O₃ exposure matched the observed O₃ dose-response functions in
 285 CLRTAP (2017). JULES was run to be as directly comparable as possible to the dose-based O₃ risk indicator used
 286 in CLRTAP (2017), using the O₃ flux per projected leaf area to top canopy sunlit leaves. Values of F_{O_3crit} came
 287 from the observations, the parameter ‘ a ’ was modified until the modelled change in response variable with
 288 cumulative uptake of O₃ above the specified threshold matched the observations (see further method details in SI
 289 section S2).

290

291 **2.3 Representation of stomatal conductance**

292

293 In JULES, g_s (m s⁻¹) is represented following the closure proposed by (Jacobs, 1994):

294

295 $g_s = 1.6RT_l \frac{A_{net}\beta}{c_a - c_i}$ (5)

296

297 In this parameterisation, c_i is unknown and in the default JULES model is calculated as in equation 6, hereafter
 298 called JAC:

299

$$300 \quad c_i = (c_a - c_*)f_0 \left(1 - \frac{dq}{dq_{crit}}\right) + c_* \quad (6)$$

301

302 β is a soil moisture stress factor, the factor 1.6 accounts for g_s being the conductance for water vapour rather than
 303 CO_2 , R is the universal gas constant ($\text{J K}^{-1} \text{mol}^{-1}$), T_l is the leaf surface temperature (K), c_a and c_i (both Pa) are the
 304 leaf surface and internal CO_2 partial pressures, respectively, c_* (Pa) is the CO_2 photorespiration compensation
 305 point, dq is the humidity deficit at the leaf surface (kg kg^{-1}), dq_{crit} (kg kg^{-1}) and f_0 are PFT specific parameters
 306 representing the critical humidity deficit at the leaf surface, and the leaf internal to atmospheric CO_2 ratio (c_i/c_a)
 307 at the leaf specific humidity deficit (Best *et al.* 2011), values are shown in Table S1.

308

309 In this work, we replace equation 6 with the closure described in Medlyn *et al.* (2011), using the key PFT specific
 310 model parameter g_l ($\text{kPa}^{0.5}$), and dq is expressed in kPa, shown in eq 7, hereafter called MED:

311

$$312 \quad c_i = c_a \left(\frac{g_l}{g_l + \sqrt{dq}} \right) \quad (7)$$

313

314 PFT specific values of the g_l parameter were derived for European vegetation from the data base of Lin *et al.*
 315 (2015) and are shown in Table S1. The g_l parameter represents the sensitivity of g_s to the assimilation rate, i.e.
 316 plant water use efficiency, and was derived as in Lin *et al.* (2015) by fitting the Medlyn *et al.*, (2011) model to
 317 observations of g_s , photosynthesis, and VPD, with no g_0 term. Hoshika *et al.* (2013) show a significant difference
 318 in the g_l parameter (higher in elevated O_3 compared to ambient) in Siebold's beech in June of their experiment.
 319 However, this is only at the start of the growing season, further measurements show no difference in this parameter
 320 between O_3 treatments. Quantifying an O_3 effect directly on g_l would require a detailed meta-analysis of empirical
 321 data on photosynthesis and g_s for different PFTs, which is currently lacking in the literature. As explained above,
 322 here we take an empirical approach to modelling plant O_3 damage, essentially by applying a reduction factor to
 323 the simulated plant photosynthesis based on observations of whole plant losses of biomass with O_3 exposure, for
 324 which there is a lot more available data (e.g. CLRTAP, 2017). The impact of the g_s model formulation is shown
 325 for two contrasting grid points (wet/dry) in central Europe (see SI section S3 for further details). We also carry
 326 out site level evaluation of the two g_s models compared to FLUXNET observations (see SI section S4).

327

328 **2.4 Model simulations for Europe**

329

330 **2.4.1 Forcing datasets**

331

332 We used the WATCH meteorological forcing data set (Weedon *et al.*, 2010; Weedon *et al.*, 2011) at $0.5^\circ \times 0.5^\circ$
 333 spatial and three hour temporal resolution for our JULES simulations. JULES interpolates this down to an hourly
 334 model time step. For this study, the climate was kept constant by recycling over the period 1901 to 1920, to allow
 335 us to fully understand the impact O_3 , CO_2 and their interaction.

336
337
338
339
340
341
342
343
344
345
346
347
348
349
350
351
352
353
354
355
356
357
358
359
360
361
362
363
364
365
366
367
368
369
370
371
372
373
374

JULES was run with prescribed annual mean atmospheric CO₂ concentrations. Pre-industrial global CO₂ concentrations (1900 to 1960) were taken from Etheridge et al. (1996), 1960 to 2002 were from Mauna Loa (Keeling and Whorf, 2004), as calculated by the Global Carbon Project (Le Quéré et al., 2016), and 2003-2050 were based on the IPCC SRES A1B scenario and were linearly interpolated to gap fill missing years (Fig. 1).

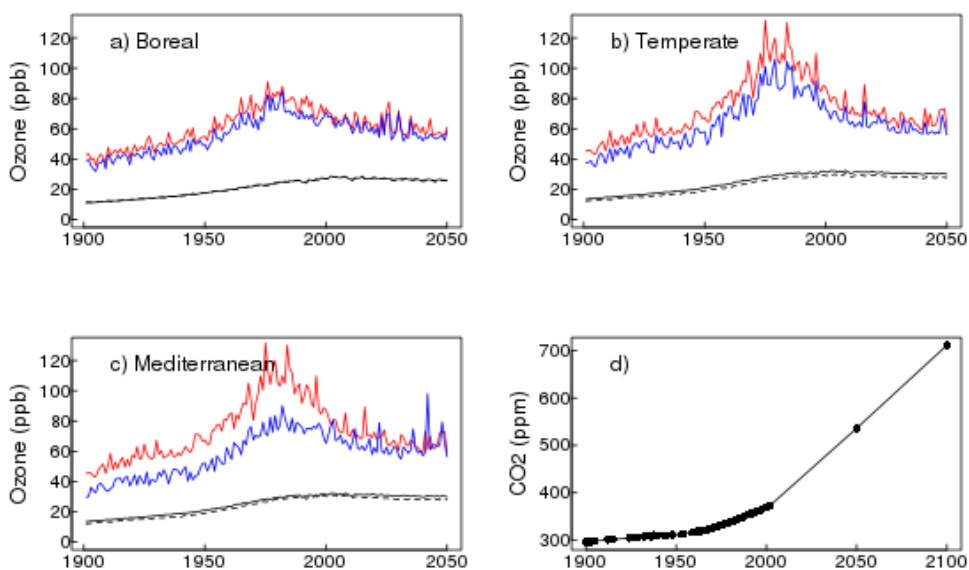
JULES was run including dynamic vegetation with a land cover mask giving the fraction of agriculture in each 0.5° x 0.5° grid cell based on the Hurtt et al. (2011) land cover database for the year 2000. The agricultural mask means that only C₃/C₄ herbaceous PFTs are allowed to grow, with no competition from other PFTs, no form of land management is simulated. By including dynamic vegetation, grid cell PFT coverage and Leaf Area Index (LAI) is a result of resource availability and simulated competition. Following a full spin-up period (to ensure equilibrium vegetation, carbon and water states), the fractional cover of each PFT changed little over the simulation period (1901 - 2050), the land cover for 2050 is shown in Fig. S1.

Tropospheric O₃ concentration was produced by the EMEP MSC-W model at 0.5° x 0.5° (Simpson et al., 2012), driven with meteorology from the regional climate model RCA3 (Kjellström et al., 2011; Samuelsson et al., 2011), which provides a downscaling of the ECHAM A1B-r3 (simulation 11 of Kjellström *et al.*, 2011). This setup (EMEP+RCA3) is also used by Langner et al. (2012a), Simpson et al. (2014a), Tuovinen et al. (2013), Franz et al. (2017) and Engardt et al. (2017), where further details and model evaluation can be found. Unfortunately, the 3-dimensional RCA3 data needed by the EMEP model was not available prior to 1960, but as in Engardt et al. (2017) the meteorology of 1900-1959 had to be approximated by assigning random years from 1960 to 1969. This procedure introduces some uncertainty of course, but Langner et al. (2012b) show that it is emissions change, rather than meteorological change, that drives modelled ozone concentrations. The emissions scenarios for 1900-2050 merge data from the International Institute of Applied System Analysis (IIASA) for 2005-2050 (the so-called ECLIPSE 4a scenario), recently revised EMEP data for 1990, and a scaling back from 1990 to 1900 using data from Lamarque et al. (2013). The EMEP model accounts for changes in BVOC emissions as a result of predicted ambient temperature changes, however as with all uncoupled modelling studies, there is no interaction between changes in leaf-level g_s , BVOCs and O₃ formation.

This study used daily mean values of tropospheric O₃ concentration from EMEP MSC-W disaggregated down to the hourly JULES model time-step. The daily mean O₃ forcing was disaggregated to follow a mean diurnal profile of O₃, this was generated from hourly O₃ output from EMEP MSC-W for the two land cover categories across the same domain as in this study. Hourly O₃ values allow for variation in the diurnal response to O₃ exposure resulting in more accurate estimation of O₃ uptake. O₃ concentrations from EMEP were calculated at canopy height for two land-cover categories: forest and grassland (Fig. S3 and Fig. S4), which are taken as surrogates for high and low vegetation, respectively. These canopy-height specific concentrations allow for the large gradients in O₃ concentration that can occur in the lowest 10s of metres, giving lower O₃ for grasslands than seen at e.g. 20 m in a forest canopy (Simpson et al., 2012; Tuovinen et al., 2009).

375 Figure 1 shows large increases in tropospheric O₃ from pre-industrial to present day (2001), this is in line with
 376 modelling studies (Young et al., 2013) and site observations (Derwent et al., 2008; Logan et al., 2012; Parrish et
 377 al., 2012), and is predominantly a result of increasing anthropogenic emissions (Young et al., 2013). Figure's S3
 378 and S4 show this large increase in ground-level O₃ concentrations from 1901 to 2001 occurs in all seasons. Present
 379 day O₃ concentration show a strong seasonal cycle, with a spring/summer peak in concentrations in the mid-
 380 latitudes of the Northern Hemisphere (Derwent et al., 2008; Parrish et al., 2012; Vingarzan, 2004). This is largely
 381 related to the seasonal cycle of photochemical O₃ production which is highest during periods of high radiation and
 382 temperature (Young et al., 2013), although increased stratospheric input is also thought to contribute (Vingarzan,
 383 2004). Anthropogenic emissions, especially NO_x, contribute to the seasonal cycle of O₃ through traffic, energy
 384 production and residential heating and cooling demands (Royal-Society, 2008). Biogenic emissions are also
 385 seasonal which contributes to the seasonal change in O₃ concentrations (Pacifico et al., 2012; Young et al., 2009),
 386 and dry deposition, driven by plant productivity also has a strong seasonal component. How the seasonality of
 387 ground level O₃ changes in the future will depend on how these multiple different drivers change and interact.
 388 Modelling studies such as Dentener et al. (2006) and Young et al. (2013) suggest that anthropogenic emissions
 389 will be the main factor controlling the evolution of future O₃ concentrations, and in the recent study of Young et
 390 al., (2013) most scenarios suggest reduced O₃ burden in the future as a result predominantly of reduced precursor
 391 emissions. Seasonally, the O₃ concentrations used in the simulations in this study show increased O₃ levels in
 392 winter and in some regions in autumn and spring in 2050 compared to present day, this may be due to reduced
 393 titration of O₃ by NO as a result of reduced NO_x emissions in the future (Royal Society, 2008). Summer O₃
 394 concentrations are lower in 2050 however, compared to 2001. Our simulations use a fixed climate, so we do not
 395 include the effect of climate change on shifting plant phenology. Therefore, our results may underestimate plant
 396 O₃ damage, since if the growing season started earlier or finished later, plants in some regions would be exposed
 397 to higher O₃ concentrations.

398
 399



400

401 **Figure 1.** Regional time series of canopy height O₃ (ppb) forcing from EMEP a) to c), and d) global atmospheric
402 CO₂ (ppm) concentration (this does not vary regionally; black dots show data points, the black line shows
403 interpolated points). Each panel for the O₃ forcing shows the regional annual average (woody PFTs, black solid
404 line; herbaceous PFTs, black dashed line) and the annual maximum O₃ concentration above: woody PFTs (red)
405 and herbaceous PFTs (blue).

406

407 2.4.2 Spin up and factorial experiments

408

409 JULES was spun-up by recycling the climate from the early part of the twentieth century (1901 to 1920) using
410 atmospheric CO₂ (296.1 ppm) and O₃ concentrations from 1901 (Fig. S3 & Fig. S4). Model spin-up was 2000
411 years by which point the carbon pools and fluxes were in steady state with zero mean net land – atmosphere CO₂
412 flux. We performed the following transient simulations for the period 1901 to 2050 with continued recycling of
413 the climate as used in the spin-up, for both high and low plant O₃ sensitivities:

414

- 415 • **O3** : Fixed 1901 CO₂, Varying O₃
- 416 • **CO2** : Varying CO₂, Fixed 1901 O₃
- 417 • **CO2 + O3** : Varying CO₂, Varying O₃

418

419 We use these simulations to investigate the direct effects of changing atmospheric CO₂ and O₃ concentrations,
420 individually and combined, on plant physiology through the twentieth century and into the future, specifically
421 over three time periods: historical (1901-2001), future (2001-2050) and over the full time series (1901-2050). See
422 the SI section S6 for calculation of the effects due to O₃, CO₂ and O₃ + CO₂. We also use paired t-test to determine
423 statistically significant differences between the different (high and low) plant O₃ sensitivities.

424

425 2.4.3 Evaluation

426 To evaluate our JULES simulations we compare mean GPP from 1991 to 2001 for each of the JULES scenarios
427 and both high and low plant O₃ sensitivities against the observation based globally extrapolated Flux Network
428 model tree ensemble (MTE) (Jung et al., 2011). We use paired t-test to determine statistically significant
429 differences in the mean responses.

430

431 3 Results

432

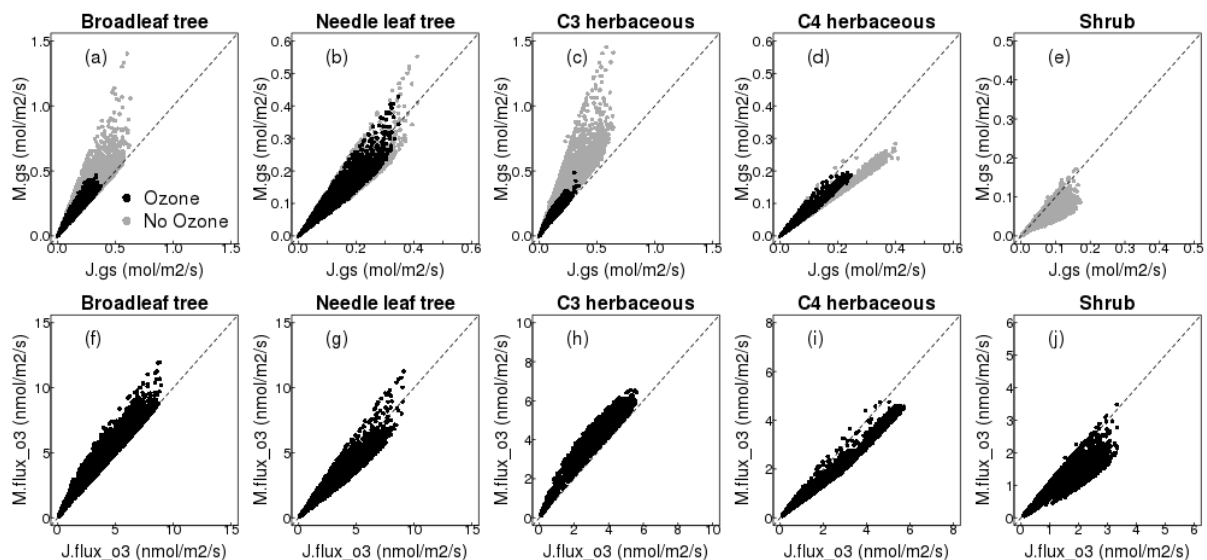
433 3.1 Impact of g_s model formulation

434

435 The impact of g_s model on simulated g_s is shown for the wet site (Fig. 2). For the broadleaf tree and C₃ herbaceous
436 PFT, the MED model simulates a larger conductance compared to the JAC model. In other words, with the MED
437 model these two PFTs are parameterised with a less conservative water use strategy, which, for the grid point
438 shown in Fig. 2, increased the annual mean leaf-level water use by 35% (±29%) and 45% (±32%), respectively.

439 In contrast, the needle leaf tree, C₄ herbaceous and shrub PFTs are parameterised with a more conservative water
 440 use strategy with the MED model, and the mean annual g_s was decreased by 13% ($\pm 12\%$), 27% ($\pm 10\%$) and 36%
 441 ($\pm 13\%$), respectively, compared to the JAC model. This comparison was also done for a dry site, and similar
 442 results were found (Fig. S6), suggesting these results are representative across the domain. The effect of g_s
 443 formulation on simulated photosynthesis was much smaller because of the lower sensitivity of the limiting rates
 444 of photosynthesis to changes in c_i in the model compared to the effect of the same change in c_i on modelled g_s
 445 (Fig. S7 & S8). Changes in leaf-level g_s impact the partitioning of simulated energy fluxes. In general, increased
 446 g_s results in increased latent heat and thus decreased sensible heat flux, and vice versa where g_s is decreased (Fig.
 447 S7 & S8). Also shown is the effect of the MED model on O₃ flux into the leaf (Fig. 2 and Fig. S6, bottom panels).
 448 For the broadleaf tree and C₃ herbaceous PFT, the MED model simulates a larger conductance and therefore a
 449 greater flux of O₃ through stomata compared to JAC, and this is indicative of the potential for greater reductions
 450 in photosynthesis (Fig. S7 & S8). The reverse is seen for the needle leaf tree, C₄ herbaceous and shrub PFTs. See
 451 SI section S4 for site level evaluation of the seasonal cycles of latent and sensible heat with both JAC and MED
 452 models compared to FLUXNET observations.

453



454

455 **Figure 2.** Comparison of simulated g_s with MED (y axis) versus JAC (x axis) for all five JULES PFTs at one grid
 456 point (lat: 48.25; lon.: 5.25) shown are hourly values for the year 2000 (see SI section S3 for further details).
 457 Shown are stomatal conductance (g_s , top row), and the flux of O₃ through the stomata (flux_o3, bottom row).

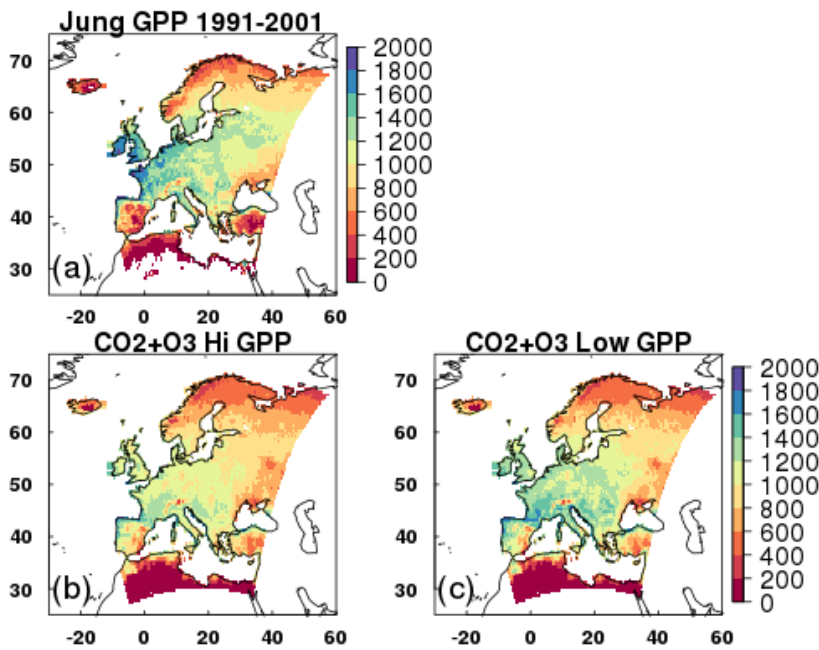
458

459 3.2 Evaluation of the JULES O₃ model

460 For all JULES scenarios similar spatial patterns of GPP are simulated compared to MTE (Fig. 3 and Fig. S10).
 461 MTE estimates a mean GPP for present day in Europe of 938 gC m² yr⁻¹ (Fig. 3). JULES tends to under-predict
 462 GPP relative to the MTE product, estimates of GPP from JULES with both transient CO₂ and O₃ give a mean
 463 across Europe of 813 gC m² yr⁻¹ (high plant O₃ sensitivity) to 881 gC m² yr⁻¹ (low plant O₃ sensitivity), both of
 464 which are significantly different to the MTE product ($t=27$, $d.f.=5750$, $p<2.2e^{-16}$ (high); $t=4.3$, $d.f.=5750$, $p<1.5e^{-$

465 ⁰⁵ (low); Fig. 3). Forcing with CO₂ alone (fixed 1901 O₃) gives a mean GPP across Europe of 900 to 923 gC m²
 466 yr⁻¹ (high and low plant O₃ sensitivity respectively), and O₃ alone (without the protective effect of CO₂) reduces
 467 estimated GPP to 732 to 799 gC m² yr⁻¹ (Fig. S10). At latitudes >45°N JULES has a tendency to under-predict
 468 MTE-GPP, and at latitudes <45°N JULES tends to over-predict MTE-GPP (Fig. S11). These regional differences
 469 are highlighted in Fig. S12, where in the Mediterranean region, JULES tends to over-predict MTE-GPP, so
 470 simulations with O₃ reduce the simulated GPP bringing it closer to MTE. In the temperate region however, JULES
 471 tends to under-estimate MTE-GPP, so the addition of O₃ reduces simulated GPP further (Fig. S12). In the boreal
 472 region, JULES under-predicts GPP, but to a lesser extent than in the temperate region, and the addition of O₃ has
 473 less impact on reducing the GPP further (Fig. S12).

474



475

476 **Figure 3.** Mean GPP (g C m² yr⁻¹) from 1991 to 2001 for a) the observationally based globally extrapolated Flux
 477 Network model tree ensemble (MTE) (Jung *et al.*, 2011); b, c) model simulations with transient CO₂ and transient
 478 O₃, high and low plant O₃ sensitivity respectively.

479

480

481 3.3 European simulations - Historical Period: 1901-2001

482

483 Over the historical period (1901-2001), the physiological effect of O₃ reduced GPP (-3% to -9%) for the low and
 484 high plant O₃ sensitivity parameterizations, respectively (Table 1). The difference in plant O₃ sensitivity was
 485 significant ($t=102.2$, $df=6270$, $p<2.2e^{-16}$). Figure 4 highlights regional variations, however, where simulated
 486 reductions in GPP are up to 20% across large areas of Europe, and up to 30% in some Mediterranean regions
 487 under the high plant O₃ sensitivity. Some Boreal and Mediterranean regions show small increases in GPP over
 488 this period, associated with O₃ induced stomatal closure enhancing water availability in these drier regions (Fig.

489 5). This allows for greater stomatal conductance later in the year when soil moisture may otherwise have been
490 limiting to growth (up to 10%, Fig. 5), and therefore higher GPP, but these regions comprise only a small area of
491 the entire domain. Indeed, over much of the Europe, O₃-induced stomatal closure led to reduced *g_s* (up to 20%)
492 across large areas of temperate Europe and the Mediterranean, and even greater reductions in some smaller regions
493 of southern Mediterranean (Fig. 6), and these are not associated with notable increases in soil moisture availability
494 (Fig. 5), resulting in depressed GPP over much of Europe as described above. Under the low plant O₃ sensitivity,
495 similar spatial patterns occur, but the magnitude of GPP change (up to -10% across much of Europe) and *g_s* change
496 (-5% to -10%) are lower compared to the high sensitivity. Over the twentieth century the land carbon sink is
497 suppressed (-2% to -6%, Table 1). Large regional variation is shown in Figure 4, with temperate and
498 Mediterranean Europe seeing a large reduction in land carbon storage, particularly under the high plant O₃
499 sensitivity (up to -15%). Combined, the physiological response to changing CO₂ and O₃ concentrations results in
500 a net loss of land carbon over the twentieth century under the high plant O₃ sensitivity (-2%, Table 1), dominated
501 by loss of soil carbon (Table S3). This reflects the large increases in tropospheric O₃ concentration observed over
502 this period (Fig. 1). Under the low plant O₃ sensitivity, the land carbon sink has started to recover by 2001 (+1.5%)
503 owing to the recovery of the soil carbon pool beyond 1901 values over this period (Table S3).

504

505 To gain perspective on the magnitude of the O₃ induced flux of carbon from the land to the atmosphere we relate
506 changes in total land carbon to carbon emissions from fossil fuel combustion and cement production for the EU-
507 28-plus countries from the data of Boden et al. (2013). We recognise that our simulation domain is slightly larger
508 than the EU28-plus as it includes a small area of western Russia so direct comparisons cannot be made, but this
509 still provides a useful measure of the size of the carbon flux. For the period 1970 to 1979 the simulated loss of
510 carbon from the European terrestrial biosphere due to O₃ effects on vegetation physiology was on average 1.32
511 Pg C (high vegetation sensitivity) and 0.71 Pg C (low vegetation sensitivity) (Table 2). This O₃ induced reduced
512 C uptake of the land surface is equivalent to around 8% to 16% of the emissions of carbon from fossil fuel
513 combustion and cement production over the same period for the EU28-plus countries (Table 2). Currently the
514 emissions data availability goes up to 2011, so over the last observable decade (2002 to 2011) this land carbon
515 loss has declined but is still equivalent to 2% to 4% of the emissions of carbon from fossil fuels and cement
516 production for the EU28-plus countries (Table 2). Therefore, the indirect O₃ effect on the land carbon sink
517 potentially represents a significant source of anthropogenic carbon.

518

519 **3.4 European simulations - Future Period: 2001-2050**

520

521 Over the 2001 to 2050 period, region-wide GPP with O₃ only changing increased marginally (+0.1% to +0.2%,
522 high and low plant O₃ sensitivity, Table 1, with a significant difference between the two plant O₃ sensitivities
523 ($t=57$, $d.f.=6270$ $p<2.2e^{-16}$)), although with large spatial variability (Fig. 4g & h). Figures S3 and S4 show that
524 despite decreased tropospheric O₃ concentrations by 2050 in summer compared to 2001 levels, all regions are
525 exposed to an increase in O₃ over the wintertime, and some regions of Europe, particularly
526 temperate/Mediterranean experience increases in O₃ concentration in spring and autumn. Therefore, although
527 increased GPP (dominantly 10%, but up to 20% in some areas) on 2001 levels is simulated across large areas of
528 Europe, decreases of up to 21% are simulated in some areas of the Mediterranean, up to 15% in some areas of the

529 boreal region and up to 27% in the temperate zone (Fig. 4g & h). When O₃ and CO₂ effects are combined,
530 simulated GPP increases (+15% to +18%, high/low plant O₃ sensitivities respectively, Table 1). This increase is
531 greater than the enhancement simulated when CO₂ affects plant growth independently, because additional O₃
532 induced stomatal closure increases soil water availability in some regions, which enhances growth more in the O₃
533 and CO₂ simulations, compared to the CO₂ only run. Nevertheless, although the percentage gain is larger, the
534 absolute value of GPP by 2050 remains lower compared to GPP with CO₂ only changing (Table S4).

535

536 Despite small increases in GPP in the O₃-only simulation, the land carbon sink continues to decline from 2001
537 levels (-0.7% to -1.6%, low and high plant O₃ sensitivity respectively, Table 1). This is because the soil and
538 vegetation carbon pools continue to lose carbon as they adjust slowly to small changes in input (GPP), i.e. the soil
539 carbon pool is not in equilibrium in 2001, and is declining in response to reduced litter input as a result of 20th C
540 O₃ impacts on GPP. Nevertheless, the negative effect of O₃ on the future land sink is markedly reduced relative
541 to the historical period. Figure 4e & f however highlights regional differences. Boreal regions and parts of central
542 Europe see minimal O₃ damage, whereas some areas of southern and northern Europe see further losses of up to
543 8% on 2001 levels. The combined O₃ and CO₂ effects are dominated by the physiological effects of changing
544 CO₂, with land carbon sink increases of up to 7% (Table 1).

545

546 **3.5 European simulations - Anthropocene: 1901-2050**

547

548 Over the Anthropocene, O₃ reduces GPP (-4% to -9%, with a significant difference between the low and high
549 plant O₃ sensitivity ($t=95$, $d.f.=6270$ $p<2.2e^{-16}$)) and land carbon storage (-3% to -7%, Table 1, Fig. S13).
550 Regionally, O₃ damage is lowest in the boreal zone, GPP decreases are largely between 5% to 8% / 2% to 4% for
551 the high/low plant O₃ sensitivity respectively, with large areas minimally affected by O₃ damage (Figure 7),
552 consistent with lower g_s of needle leaf trees that dominate this region, and so lower O₃ uptake (Fig. S14 & S15).
553 In the temperate region, O₃ damage is extensive with reductions in GPP dominantly from 10% to 15% for the low
554 and high plant O₃ sensitivity respectively. Across significant areas of this region reductions in GPP are up to 20%
555 under high plant O₃ sensitivity (Figure 7). In the Mediterranean region, O₃ damage reduces GPP by 5% to 15% /
556 3% to 6% for the high/low plant O₃ sensitivity respectively, with some areas seeing greater losses of up to 20%
557 under the high plant O₃ sensitivity, but this is less extensive than that seen in the temperate zone (Figure 7). In
558 these drier regions, O₃ induced stomatal closure can increase available soil moisture (Fig. S14 & S15).

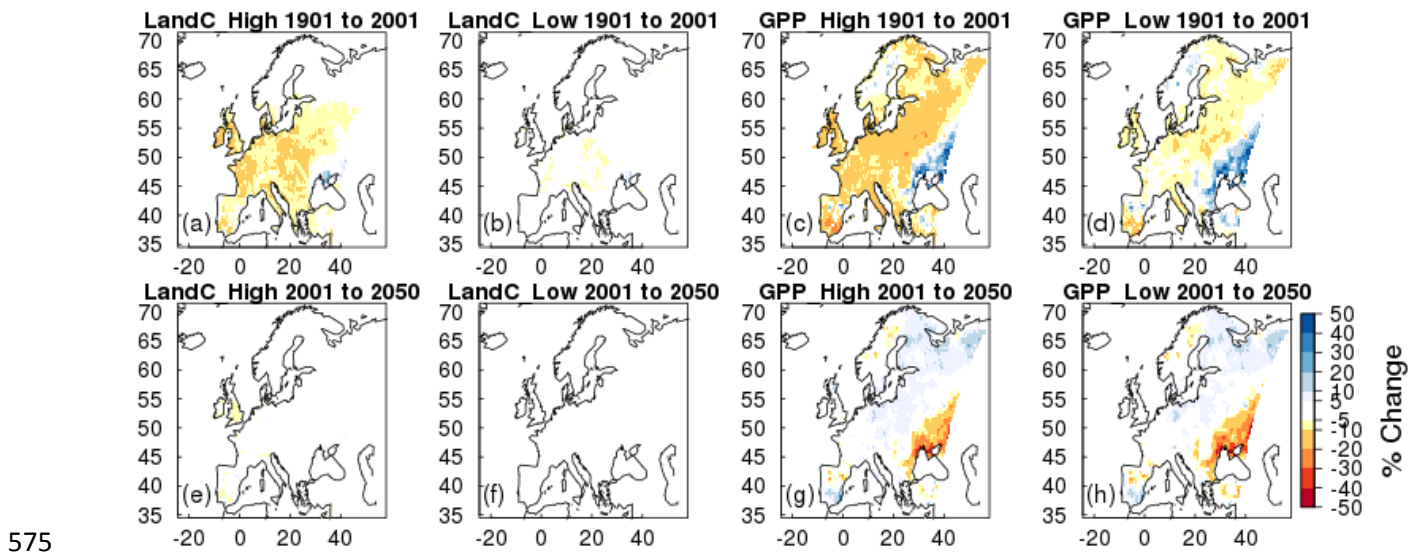
559

560 Varying CO₂ and O₃ together shows that CO₂ induced stomatal closure can help alleviate O₃ damage by reducing
561 the uptake of O₃ (Table S6). In these simulations, CO₂-induced stomatal closure was found to offset O₃-suppression
562 of GPP, such that GPP by 2050 is 3% to 7% lower due to O₃ exposure, rather than 4% to 9% lower in the absence
563 of increasing CO₂ (Table S6). Figure 6 shows this spatially, O₃ damage is reduced when the effect of atmospheric
564 CO₂ on stomatal closure is accounted for, however despite this, the land carbon sink and GPP remain significantly
565 reduced due to O₃ exposure.

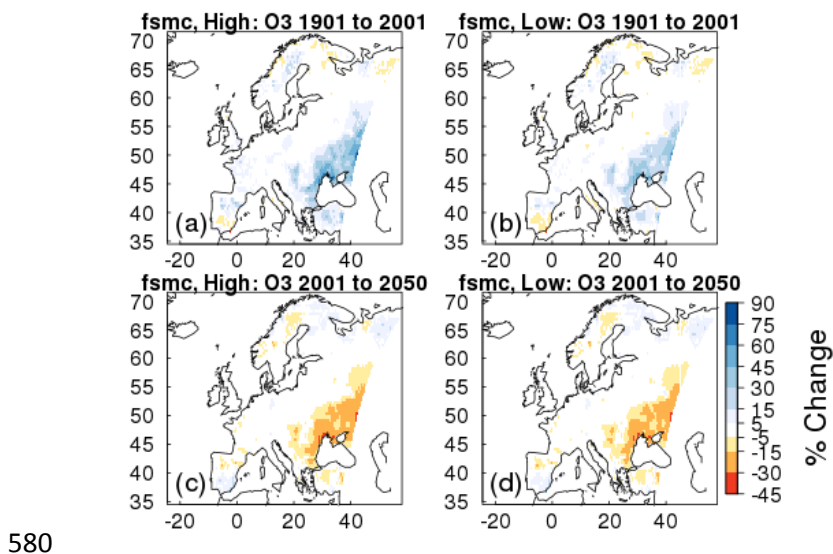
566

567 Over the Anthropocene, changing O₃ and CO₂ in tandem results in an increase in European land carbon uptake
568 (+5% to +9%), and an increase in GPP (+20% to +23%) by 2050 for the high and low plant O₃ sensitivity,

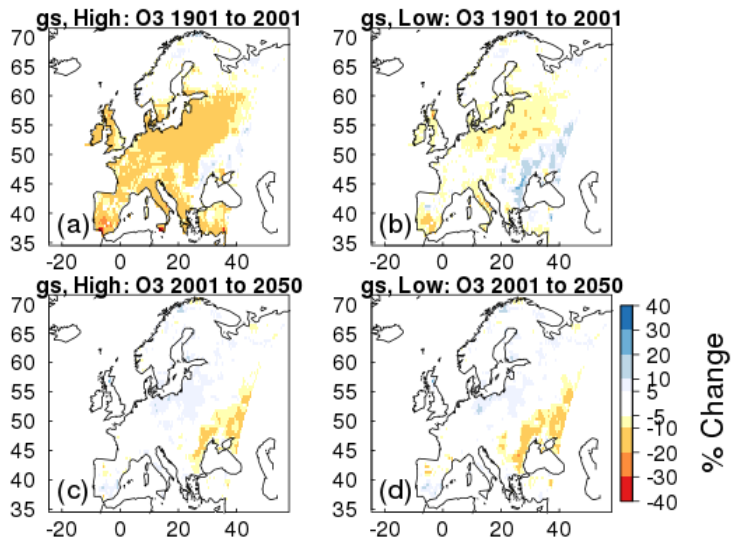
569 respectively (Table 1). Nevertheless, despite this increase there remains a large negative impact of O₃ on the
 570 European land carbon sink (Fig. S13). By 2050 the simulated enhancement of land carbon and GPP in response
 571 to elevated CO₂ alone is reduced by 3% to 6% (land carbon) and 4% to 9% (GPP) for the low and high plant O₃
 572 sensitivity respectively, when O₃ is also accounted for (Table 1). This is a large reduction in the ability of the
 573 European terrestrial biosphere to sequester carbon.
 574



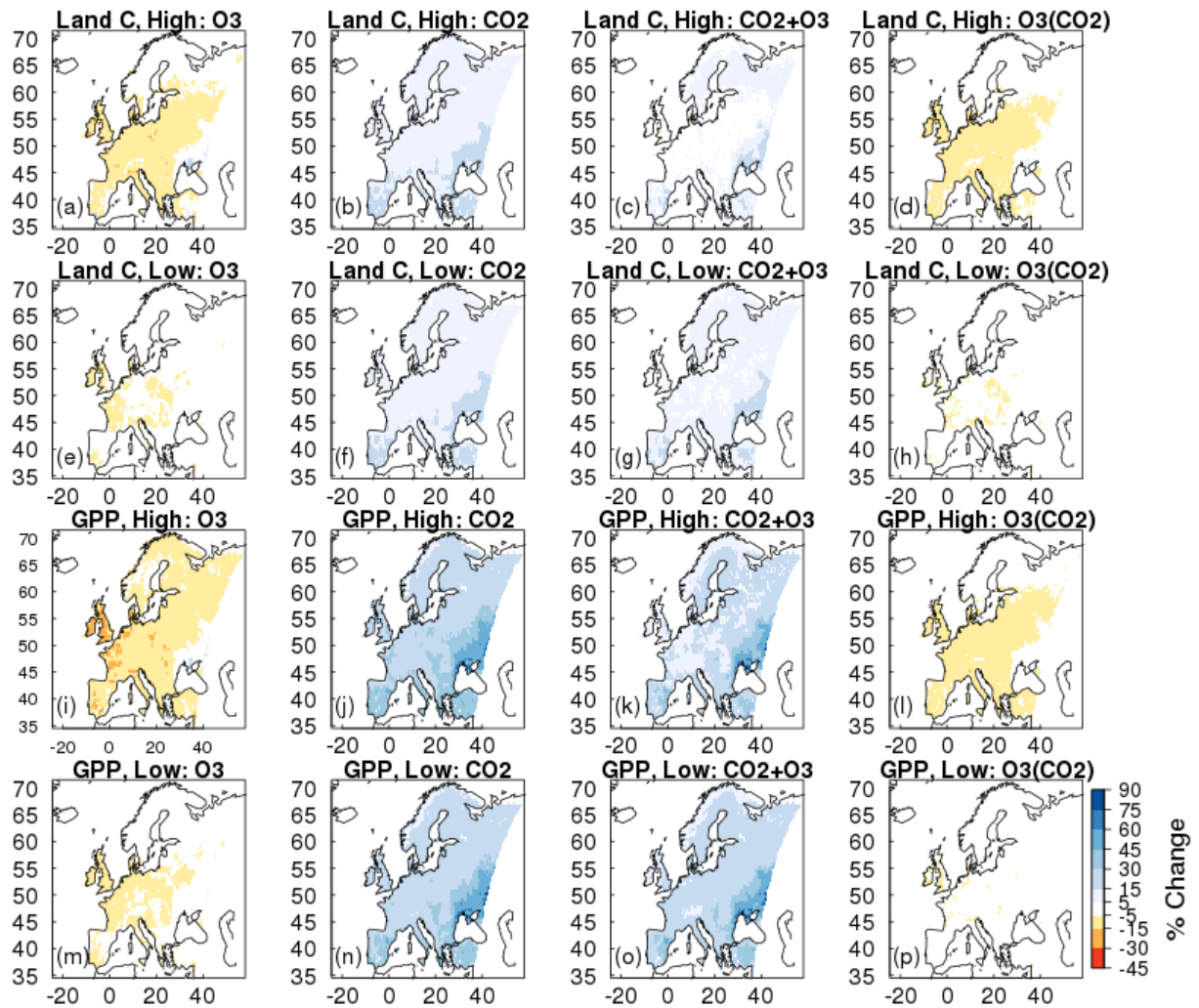
576 **Figure 4.** Simulated percentage change in total carbon stocks (Land C) and gross primary productivity (GPP) due to
 577 O₃ effects at fixed pre-industrial atmospheric CO₂ concentration. Changes are shown for the periods 1901 to
 578 2001, and 2001 to 2050 for the high and low plant O₃ sensitivity.
 579



581 **Figure 5.** Simulated percentage change in plant available soil moisture (*fsmc*) due to O₃ effects at fixed pre-
582 industrial atmospheric CO₂ concentration. Changes are shown for the periods 1901 to 2001, and 2001 to 2050 for
583 the high and low plant O₃ sensitivity.
584



585
586 **Figure 6.** Simulated percentage change in stomatal conductance (*g_s*) due to O₃ effects at fixed pre-industrial
587 atmospheric CO₂ concentration. Changes are shown for the periods 1901 to 2001, and 2001 to 2050 for the high
588 and low plant O₃ sensitivity.
589



590

591 **Figure 7.** Simulated percentage change in total carbon stocks (Land C) and gross primary productivity (GPP) due
 592 to i) (a, e, i, m) O₃ effects at fixed pre-industrial atmospheric CO₂ concentration (O₃), ii) (b, f, j, n) CO₂ fertilisation
 593 at fixed pre-industrial O₃ concentration (CO₂), iii) (c, g, k, o) the interaction between O₃ and CO₂ effects (CO₂ +
 594 O₃) iv) (d, h, l, p) O₃ effects with changing atmospheric CO₂ concentration (i.e. O₃ damage accounting for the
 595 effect of CO₂ induced stomatal closure; O₃(CO₂)). Changes are depicted for the periods 1901 to 2050 for high and
 596 lower ozone plant sensitivity.

597

598

599

600

601

602

603

	High Plant O₃ Sensitivity					
	1901 - 2001		2001 - 2050		1901 - 2050	
	GPP (Pg C yr ⁻¹)	Land C (Pg C)	GPP (Pg C yr ⁻¹)	Land C (Pg C)	GPP (Pg C yr ⁻¹)	Land C (Pg C)
Value in 1901:	9.05	167	-	-	9.05	167
Absolute Change:						
O₃	-0.81	-9.21	0.01	-2.44	-0.80	-11.65
CO₂	1.16	4.24	1.42	12.98	2.58	17.22
CO₂ + O₃	0.13	-3.28	1.66	11.11	1.79	7.83
% Change:						
O₃	-8.95	-5.51	0.12	-1.55	-8.84	-6.98
CO₂	12.82	2.54	13.91	7.58	28.51	10.31
CO₂ + O₃	1.44	-1.96	18.08	6.79	19.78	4.69
	Low Plant O₃ Sensitivity					
	1901 - 2001		2001 - 2050		1901 - 2050	
	GPP (Pg C yr ⁻¹)	Land C (Pg C)	GPP (Pg C yr ⁻¹)	Land C (Pg C)	GPP (Pg C yr ⁻¹)	Land C (Pg C)
Value in 1901:	9.34	167.5	-	-	9.34	167.5
Absolute Change:						
O₃	-0.30	-3.59	0.02	-1.07	-0.40	-4.66
CO₂	1.15	6.43	1.35	13.14	2.50	19.57
CO₂ + O₃	0.65	2.50	1.50	12.35	2.15	14.85
% Change:						
O₃	-3.21	-2.14	0.22	-0.65	-4.28	-2.78
CO₂	12.31	3.84	12.87	7.55	26.77	11.68
CO₂ + O₃	6.96	1.49	15.02	7.26	23.02	8.87

604

605 **Table 1.** Simulated changes in the European land carbon cycle due to changing O₃ and CO₂ concentrations
606 (independently and together). Shown are changes in total carbon stocks (Land C) and gross primary productivity
607 (GPP), over three different periods (historical: 1901 to 2001, future: 2001 to 2050, and Anthropocene: 1901 to
608 2050). Absolute (top) and relative (bottom) differences are shown. For 2001 to 2050, please refer to Table S4 for
609 the initial value for each run. See the SI for details of the estimation of the O₃ and CO₂ effects and their interaction.

610

611

612

613

614

615

616

617

618

619

	Mean (Pg C)				
	1970-1979	1980-1989	1990-1999	2000-2009	2002-2011
Modelled O₃ effect on land C sink :					
Higher sensitivity	-1.32	-1.01	-0.97	-0.53	-0.50
Low sensitivity	-0.71	-0.58	-0.50	-0.29	-0.26
Sum of C emissions from fossil fuel combustion and cement production (Pg C)					
	8.39	8.63	12.26	12.83	12.75
C lost from O₃ effect as a % of fossil fuel and cement emissions (%):					
Higher sensitivity	-15.73	-11.70	-7.91	-4.13	-3.92
Low sensitivity	-8.46	-6.72	-4.08	-2.26	-2.04

620

621 **Table 2.** Simulated change in total land carbon due to O₃ damage with changing atmospheric CO₂ concentration
622 for the two vegetation sensitivities. The sum of carbon emissions for each decade from fossil fuel combustion and
623 cement production for the EU-28 countries plus Albania, Bosnia and Herzegovina, Iceland, Belarus, Serbia,
624 Moldova, Norway, Turkey, Ukraine, Switzerland and Macedonia (EU28-plus) are shown, the data is from Boden
625 *et al.*, 2013. The simulated change in land carbon as a result of O₃ damage is depicted as a percentage of the EU28-
626 plus emissions to demonstrate the magnitude of the additional source of carbon to the atmosphere from plant O₃
627 damage.

628

629 4 Discussion

630

631 4.1 Comparison of g_s models

632

633 Comparison of the new g_s model implemented in this study (MED) with the g_s model currently used as standard
634 in JULES (JAC) revealed large differences in leaf-level g_s for each PFT, principally as a result of the data-based
635 parameterisation of the new model. Leaf-level water use increased for the broadleaf tree and C₃ herbaceous PFTs
636 using the MED model compared to JAC, but decreased for the needle leaf tree, C₄ herbaceous and shrub PFTs
637 which displayed a more conservative water use strategy compared to the Jacobs parameterisation. These changes
638 are in line with the work of De Kauwe *et al.* (2015) who found a reduction in annual transpiration for evergreen
639 needle leaf, tundra and C₄ grass regions when implementing the Medlyn g_s model into the Australian land surface
640 scheme CABLE. Changes in leaf-level g_s in this study resulted in differences in latent and sensible heat fluxes.
641 Changes in the partitioning of energy fluxes at the land surface could have consequences for the intensity of
642 heatwaves (Cruz *et al.*, 2010; Kala *et al.*, 2016), runoff (Betts *et al.*, 2007; Gedney *et al.*, 2006) and rainfall patterns
643 (de Arellano *et al.*, 2012), although fully coupled simulations would be necessary to detect these effects. The
644 differences in simulated g_s led to differences in uptake of O₃ between the two models because the leaf-level rate
645 of g_s is the predominant determinant of the flux of O₃ through stomata. Higher O₃ uptake is indicative of greater
646 damage. Therefore, given that C₃ herbaceous vegetation is the dominant land cover class across the European
647 domain used in this study, this suggests a greater O₃ impact for Europe would be simulated with MED model
648 compared to JAC.

649 **4.2 Lower than expected O₃ damage?**

650

651 The impact of O₃ on present day European GPP simulated in this study is slightly lower compared to previous
652 modelled estimates. Our estimates suggest present day O₃ reduced GPP by 3% to 9% on average across Europe
653 and NPP by 5% to 11% (Table S3). Anav et al. (2011) simulated a 22% reduction of GPP across Europe for 2002
654 using the ORCHIDEE model. Present day O₃ exposure reduced GPP by 10% to 25% in Europe, and 10.8%
655 globally in the study by Lombardozzi et al. (2015) using the Community land model (CLM). O₃ reduced NPP by
656 11.2% in Europe from 1989 to 1995 using the Terrestrial Ecosystem Model (TEM) (Felzer et al., 2005). Globally,
657 concentrations of O₃ predicted for 2100 reduced GPP by 14% to 23% using a former parameterisation of O₃
658 sensitivity in JULES (Sitch et al., 2007). The recent study by Franz et al. (2017) showed mean GPP declined by
659 4.7% over the period 2001 to 2010 using the OCN model over the same European domain used in this study.
660 These similar results are likely the result of using the same domain, and, more importantly, O₃ forcing produced
661 by the same model (EMEP MSC-W).

662

663 **4.3 Impacts of O₃ at the land surface**

664

665 In this study, O₃ has a detrimental effect on the size of the land carbon sink for Europe. This is primarily through
666 a decrease in the size of the soil carbon pool as a result of reduced litter input to the soil, consistent with reduced
667 GPP/NPP. Field studies show that in some regions of Europe, soil carbon stocks are decreasing (Bellamy et al.,
668 2005;Capriel, 2013;Heikkinen et al., 2013;Sleutel et al., 2003). The study of Bellamy et al. (2005), for example,
669 showed that carbon was lost from soils across England and Wales between 1978 to 2003 at a mean rate of 0.6%
670 per year with little effect of land use on the rate of carbon loss, suggesting a possible link to climate change. It is
671 understood that climate change is likely to affect soil carbon turnover. Increased temperatures increase microbial
672 decomposition activity in the soil, and therefore increase carbon losses through higher rates of respiration (Cox et
673 al., 2000;Friedlingstein et al., 2006;Jones et al., 2003). However, some studies have found that O₃ can decrease
674 soil carbon content. Talhelm et al. (2014), for example, found O₃ reduced carbon content in near surface mineral
675 soil of forest soils exposed to 11 years of O₃ fumigation. Hofmockel et al. (2011) found elevated O₃ reduced the
676 carbon content in more stable soil organic matter pools, and Loya et al. (2003) showed that the fraction of soil
677 carbon formed in forest soils over a 4 year experimental period when fumigated with both CO₂ and O₃ was reduced
678 by 51% compared to the soil fumigated with CO₂ alone. It is agreed that amongst other factors that change with
679 O₃ exposure such as litter quality and composition, reduced litter quantity also has significant detrimental
680 consequences for soil carbon stocks (Andersen, 2003;Lindroth, 2010;Loya et al., 2003). Results from this study
681 therefore suggest that increasing tropospheric O₃ may be a contributing factor to the declining soil carbon stocks
682 observed across Europe as a result of reduced litter input to the soil carbon pool consistent with reduced NPP.

683

684 We acknowledge, however, that our model simulations do not include coupling of Nitrogen and Carbon cycles,
685 or land management practices. Although we include a representation of agricultural regions through the model
686 calibration against the wheat O₃ sensitivity function (CLRTAP, 2017), wheat is known to be one of the most O₃
687 sensitive crop species. As with all uncoupled modelling studies, a change in g_s and flux will impact the O₃
688 concentration itself. Therefore adopting the Medlyn formulation with a higher g_s and subsequently higher O₃ flux

689 for broadleaf and C₃ PFTs (Fig 2) would lead to reduced O₃ concentration, which in turn would act to dampen the
690 effect of higher g_s on O₃ flux. Essentially this study provides an ‘upper bound’ as in the high plant O₃ sensitivity
691 scenario, all C₃/C₄ fractional cover uses the wheat O₃ sensitivity. Additionally, this version of JULES does not
692 have a crop module; it has no land management practices such as harvesting, ploughing or crop rotation –
693 processes which may have counteracting effects on the land carbon sink. Further, without a coupled Carbon and
694 Nitrogen cycle, it is likely that the CO₂ fertilisation response of GPP and the land carbon sink is over estimated in
695 some regions of our simulations since nitrogen availability limits terrestrial carbon sequestration of natural
696 ecosystems in the temperate and boreal zone (Zaehle, 2013). This would have consequences for our modelled O₃
697 impact, particularly into the future where the large CO₂ fertilisation effect was responsible for partly offsetting
698 the negative impact of O₃. Although in our simulations a high fraction of land cover is agricultural which we
699 assume would be optimally fertilised. Nevertheless, we emphasise that this study provides a sensitivity assessment
700 of the impact of plant O₃ damage on GPP and the land carbon sink.

701

702 Another caveat we fully acknowledge is that at the leaf-level JULES is parameterised to reduce g_s with O₃
703 exposure. Whilst this response is commonly observed (Wittig et al., 2007; Ainsworth et al., 2012), there is evidence
704 to suggest that O₃ impairs stomata in some species, making them non-responsive to environmental stimuli (Hayes
705 et al., 2012; Hoshika et al., 2012a; Mills et al., 2009; Paoletti and Grulke, 2010). In drought conditions the
706 mechanism is thought to involve O₃ stimulated ethylene production which interferes with the stomatal response
707 to ABA signalling (Wilkinson and Davies, 2009; Wilkinson and Davies, 2010). Such stomatal sluggishness can
708 result in higher O₃ uptake and injury, increased water-loss, and therefore greater vulnerability to environmental
709 stresses (Mills et al., 2016). McLaughlin (2007a; 2007b) and Sun et al. (2012) provide evidence of increased
710 transpiration and reduced streamflow in forests at the regional scale in response to ambient levels of O₃, and
711 suggest this could increase the frequency and severity of droughts. (Hoshika et al., 2012b) Hoshika et al 2012
712 however found that despite sluggish stomatal control in O₃ exposed trees, whole tree water use was lower in these
713 trees because of lower gas exchange and premature leaf shedding of injured leaves. To our knowledge, the study
714 of Hoshika et al. (2015) is the first to include an explicit representation of sluggish stomatal control in a land-
715 atmosphere model, they show that sluggish stomatal behaviour has implications for carbon and water cycling in
716 ecosystems. However, it is by no means a ubiquitous response, and it is not fully understood which species respond
717 this way and under what conditions (Mills et al., 2016; Wittig et al., 2007). Nevertheless, this remains an important
718 area of future work.

719

720 The calculation of O₃ deposition in the EMEP model uses the stomatal conductance formulation presented in
721 Emberson et al. (2000; 2001), which depends on temperature, light, humidity and soil moisture (commonly
722 referred to as DO₃SE). Because we link two different model systems, the g_s values in the EMEP model differ from
723 those obtained using the Medlyn formulation. We acknowledge this inconsistency as a caveat of our study,
724 however comparison of g_{max} (maximum g_s) values from both models (EMEP and JULES) suggests the
725 differences are small for deciduous forest (EMEP 150-200, JULES ~180, all units in mmole O₃/m² (PLA)/s), and
726 C₃/C₄ crops (EMEP 270-300, JULES ~260-390 – the dominant land cover in our simulations), but are larger for
727 coniferous forest (EMEP 140-200, JULES ~60-70) and shrubs (EMEP 60-200, JULES 360-390). The role of
728 EMEP in this study is not to provide g_s , however, but to provide O₃ at the top of the vegetation canopy. The main

729 driver of such O₃ levels is the regional-scale production and transport of O₃, and the main impact of g_s is in
730 affecting the vertical O₃ gradients just above the plant canopy. Differences in g_s are known to have minimal impact
731 on canopy-top O₃ for trees, mainly due to the efficient turbulent mixing above tall canopies, but also due to non-
732 stomatal sink processes. For shorter vegetation, substantial O₃ gradients, driven by deposition, occur in the lowest
733 10s of metres of the atmosphere, and stomatal sinks (as given by g_s) can have a significant role. However,
734 calculations of such gradients made with the EMEP model for CLRTAP (2017) showed that differences amounted
735 to only ca. 10% when comparing O₃ concentrations at 1m height above high-g_s crops compared to moderate-g_s
736 (g_{max} = 450 and 270 mmole O₃/m² (PLA)/s respectively), therefore this uncertainty is small.

737

738 These offline simulations show the sensitivity of GPP and the land carbon sink to tropospheric O₃, suggesting that
739 O₃ is an important predictor of future GPP and the land carbon store across Europe. There are uncertainties in our
740 estimates however from the use of uncoupled tropospheric chemistry, meteorology and stomatal function. For
741 example, increased frequency of drought in the future would reduce stomatal conductance (assuming no sluggish
742 stomatal response) and thus O₃ uptake. Since our offline simulations do not include this feedback it is possible the
743 O₃ effect is over estimated here. Given the complexity of potential interactions and feedbacks it remains difficult
744 to diagnose the importance of individual factors (e.g. the direct physiological response) in a fully coupled
745 simulation. Once the importance of a process is demonstrated offline, it provides evidence of the need to
746 incorporate such process in coupled regional and global simulations.

747

748 **4.4 O₃ as a missing component of carbon cycle assessments?**

749

750 Comprehensive analyses of the European carbon balance suggest a large biogenic carbon sink (Janssens et al.,
751 2003;Luyssaert et al., 2012;Schulze et al., 2009). However, estimates are hampered by large uncertainties in key
752 components of the land carbon balance, such as estimates of soil carbon gains and losses (Ciais et al.,
753 2010;Janssens et al., 2003;Schulze et al., 2009;Schulze et al., 2010). We suggest that the effect of O₃ on plant
754 physiology is a contributing factor to the decline in soil carbon stores observed across Europe, and as such this O₃
755 effect is a missing component of European carbon cycle assessments. Over the Anthropocene, our results show
756 elevated O₃ concentrations reduce the amount of carbon that can be stored in the soil by 3% to 9% (low and high
757 plant O₃ sensitivity, respectively), which almost completely offsets the beneficial effects of CO₂ fertilisation on
758 soil carbon storage under the high plant O₃ sensitivity . This would contribute to a change in the size of a key
759 carbon sink for Europe, and is particularly important when we consider the evolution of the land carbon sink into
760 the future given the impact of O₃ on soil carbon sequestration and the high uncertainty of future tropospheric O₃
761 concentrations. Schulze et al. (2009) and Luyssaert et al. (2012) extended their analysis of the European carbon
762 balance to include additional non-CO₂ greenhouse gases (CH₄ and N₂O). Both studies found that emissions of
763 these offset the biogenic carbon sink, reducing the climate mitigation potential of European ecosystems. This
764 highlights the importance of accounting for all fluxes and stores in carbon/greenhouse gas balance assessments,
765 of which O₃ and its indirect effect on the CO₂ flux via direct effects on plant physiology is currently missing.

766

767 **4.5 The interaction between O₃ and CO₂**

768

769 We looked at the interaction between CO₂ and O₃ effects. Our results support the hypothesis that elevated
770 atmospheric CO₂ provides some protection against O₃ damage because of lower g_s that reduces uptake of O₃
771 through stomata (Harmens et al., 2007; Wittig et al., 2007). In the present study, reductions in GPP and the land
772 carbon store due to O₃ exposure were lower when simulated with concurrent changes in atmospheric CO₂. Despite
773 acclimation of photosynthesis after long-term exposure to elevated atmospheric CO₂ of field grown plants
774 (Ainsworth and Long, 2005; Medlyn et al., 1999), there is no evidence to suggest that g_s acclimates (Ainsworth et
775 al., 2003; Medlyn et al., 2001). This suggests the protective effect of elevated atmospheric CO₂ against O₃ damage
776 will be sustained in the long term. However, although meta-analysis suggest a general trend of reduced g_s with
777 elevated CO₂ (Ainsworth and Long, 2005; Medlyn et al., 1999), this is not a universal response. Stomatal responses
778 on exposure to elevated CO₂ with FACE treatment varied with genotype and growth stage in a fast-growing poplar
779 community (Bernacchi et al., 2003; Tricker et al., 2009). In other mature forest stands, limited stomatal response
780 to elevated CO₂ was observed after canopy closure (Ellsworth, 1999; Uddling et al., 2009). Also, some studies
781 found that stomatal responses to CO₂ were significant only under high atmospheric humidity (Cech et al.,
782 2003; Leuzinger and Körner, 2007; Wullschleger et al., 2002). These examples illustrate that stomatal responses to
783 elevated atmospheric CO₂ are not universal, and as such the protective effect of CO₂ against O₃ injury cannot be
784 assumed for all species, at all growth stages under wide ranging environmental conditions.

785

786 **5 Conclusion**

787

788 What is abundantly clear is that plant responses to both CO₂ and O₃ are complicated by a host of factors that are
789 only partly understood, and it remains difficult to identify general, global patterns given that effects of both gases
790 on plant communities and ecological interactions are highly context and species specific (Ainsworth and Long,
791 2005; Fuhrer et al., 2016; Matyssek et al., 2010b). This study quantifies the sensitivity of the land carbon sink for
792 Europe and GPP to changing concentrations of atmospheric CO₂ and O₃ from 1901 to 2050. We have used a state
793 of the art land surface model calibrated for European vegetation to give our best estimates of this sensitivity within
794 the limits of data availability to calibrate the model for O₃ sensitivity, current knowledge and model structure. In
795 summary, this study has shown that potential gains in terrestrial carbon sequestration over Europe resulting from
796 elevated CO₂ can be partially offset by concurrent rises in tropospheric O₃ over 1901-2050. Specifically, we have
797 shown that the negative effect of O₃ on the land carbon sink was greatest over the twentieth century, when O₃
798 concentrations increased rapidly from pre-industrial levels. Over this period soil carbon stocks were diminished
799 over agricultural areas, consistent with reduced NPP and litter input. This loss of soil carbon was largely
800 responsible for the decrease in the size of the land carbon sink over Europe. The O₃ effect on the land carbon store
801 and flux was reduced into the future as CO₂ concentration rose considerably and changes in O₃ concentration were
802 less pronounced. However, there remained a large cumulative negative impact on the land carbon sink for Europe
803 by 2050. The interaction between the two gases was found to reduce O₃ injury owing to reduced stomatal opening
804 in elevated atmospheric CO₂. However, primary productivity and land carbon storage remained suppressed by
805 2050 due to plant O₃ damage. Expressed as a percentage of the emissions from fossil fuel and cement production
806 for the EU28-plus countries, the carbon emissions from O₃-induced plant injury are a source of anthropogenic
807 carbon previously not accounted for in carbon cycle assessments. Our results demonstrate the sensitivity of
808 modelled terrestrial carbon dynamics to the direct effect of tropospheric O₃ and its interaction with atmospheric

809 CO₂ on plant physiology, demonstrating this process is an important predictor of future GPP and trends in the
810 land-carbon sink. Nevertheless, this process remains largely unconsidered in regional and global climate model
811 simulations that are used to model carbon sources and sinks and carbon-climate feedbacks.

812

813

814

815 **Data availability**

816

817 The JULES model can be downloaded from the Met Office Science Repository Service
818 (<https://code.metoffice.gov.uk/trac/jules> - see here for a helpful how to [http://jules.jchmr.org/content/getting-](http://jules.jchmr.org/content/getting-started)
819 started). Model output data presented in this paper and the exact version of JULES with namelists are available
820 upon request from the corresponding author.

821

822 **Supplementary Information**

823

824 Supplementary_Information_Oliver_et_al.docx

825

826 **Competing Interests**

827 The authors declare that they have no conflict of interest

828

829 **Acknowledgements**

830

831 RJO and LMM were supported by the EU FP7 (ECLAIRE, 282910) and JWCRP (UKESM, NEC05816). This
832 work was also supported by EMEP under UNECE. SS and LMM acknowledge the support of the NERC
833 SAMBBA project (NE/J010057/1). The UK Met Office contribution was funded by BEIS under the Hadley Centre
834 Climate Programme (GA01101). GAF also acknowledges funding from the EU's Horizon 2020 research and
835 innovation programme (CRESCENDO, 641816). We also thank Magnuz Engardt of SMHI for providing the
836 RCA3 climate dataset.

837

838 **References**

839

840 Ainsworth, E., and Long, S.: What have we learned from 15 years of free-air CO₂ enrichment (FACE)?
841 A meta-analytic review of the responses of photosynthesis, canopy properties and plant production
842 to rising CO₂, *New Phytologist*, 165, 351-372, 2005.

843 Ainsworth, E. A., Davey, P. A., Hymus, G. J., Osborne, C. P., Rogers, A., Blum, H., Nosberger, J., and
844 Long, S. P.: Is stimulation of leaf photosynthesis by elevated carbon dioxide concentration
845 maintained in the long term? A test with *Lolium perenne* grown for 10 years at two nitrogen
846 fertilization levels under Free Air CO₂ Enrichment (FACE), *Plant, Cell and Environment*, 26, 705-714,
847 2003.

848 Ainsworth, E. A.: Rice production in a changing climate: a meta-analysis of responses to elevated
849 carbon dioxide and elevated ozone concentration, *Global Change Biology*, 14, 1642-1650,
850 10.1111/j.1365-2486.2008.01594.x, 2008.

851 Ainsworth, E. A., Yendrek, C. R., Sitch, S., Collins, W. J., and Emberson, L. D.: The Effects of
852 Tropospheric Ozone on Net Primary Productivity and Implications for Climate Change, *Annual*
853 *Review of Plant Biology*, 63, 637-661, doi:10.1146/annurev-arplant-042110-103829, 2012.

854 Anav, A., Menut, L., Khvorostyanov, D., and Viovy, N.: Impact of tropospheric ozone on the Euro-
855 Mediterranean vegetation, *Global change biology*, 17, 2342-2359, 2011.

856 Andersen, C. P.: Source–sink balance and carbon allocation below ground in plants exposed to
857 ozone, *New Phytologist*, 157, 213-228, 10.1046/j.1469-8137.2003.00674.x, 2003.

858 Arneth, A., Harrison, S. P., Zaehle, S., Tsigaridis, K., Menon, S., Bartlein, P. J., Feichter, J., Korhola, A.,
859 Kulmala, M., O'Donnell, D., Schurgers, G., Sorvari, S., and Vesala, T.: Terrestrial biogeochemical
860 feedbacks in the climate system, *Nature Geosci*, 3, 525-532,
861 http://www.nature.com/ngeo/journal/v3/n8/supinfo/ngeo905_S1.html, 2010.

862 Avnery, S., Mauzerall, D. L., Liu, J., and Horowitz, L. W.: Global crop yield reductions due to surface
863 ozone exposure: 1. Year 2000 crop production losses and economic damage, *Atmospheric*
864 *Environment*, 45, 2284-2296, <https://doi.org/10.1016/j.atmosenv.2010.11.045>, 2011.

865 Baig, S., Medlyn, B. E., Mercado, L. M., and Zaehle, S.: Does the growth response of woody plants to
866 elevated CO₂ increase with temperature? A model-oriented meta-analysis, *Global Change Biology*,
867 21, 4303-4319, 10.1111/gcb.12962, 2015.

868 Bellamy, P. H., Loveland, P. J., Bradley, R. I., Lark, R. M., and Kirk, G. J.: Carbon losses from all soils
869 across England and Wales 1978–2003, *Nature*, 437, 245-248, 2005.

870 Bernacchi, C. J., Calfapietra, C., Davey, P. A., Wittig, V. E., Scarascia-Mugnozza, G. E., Raines, C. A.,
871 and Long, S. P.: Photosynthesis and stomatal conductance responses of poplars to free-air CO₂
872 enrichment (PopFACE) during the first growth cycle and immediately following coppice., *New*
873 *Phytologist*, 159, 609-621, 2003.

874 Best, M. J., Pryor, M., Clark, D. B., Rooney, G. G., Essery, R. L. H., Menard, C. B., Edwards, J. M.,
875 Hendry, M. A., Porson, N., Gedney, N., Mercado, L. M., Sitch, S., Blyth, E., Boucher, O., Cox, P. M.,
876 Grimmond, C. S. B., and Harding, R. J.: The Joint UK Land Environment Simulator (JULES), Model
877 description - Part 1: Energy and water fluxes, *Geoscientific Model Development Discussions*, 4, 595-
878 640, 10.5194/GMDD-4-595-2011, 2011.

879 Betts, R. A., Boucher, O., Collins, M., Cox, P. M., Falloon, P. D., Gedney, N., Hemming, D. L.,
880 Huntingford, C., Jones, C. D., and Sexton, D. M.: Projected increase in continental runoff due to plant
881 responses to increasing carbon dioxide, *Nature*, 448, 1037-1041, 2007.

882 Boden, T. A., Marland, G., and Andres, R. J.: Global, Regional, and National Fossil-Fuel CO₂ Emissions,
883 Oak Ridge National Laboratory, U.S. Department of Energy, Oak Ridge, Tenn., USA, 2013.

884 Büker, P., Feng, Z., Uddling, J., Briolat, A., Alonso, R., Braun, S., Elvira, S., Gerosa, G., Karlsson, P. E.,
885 Le Thiec, D., Marzuoli, R., Mills, G., Oksanen, E., Wieser, G., Wilkinson, M., and Emberson, L. D.: New
886 flux based dose-response relationships for ozone for European forest tree species, *Environmental*
887 *Pollution*, 163-174, 2015.

888 Calvete-Sogo, H., Elvira, S., Sanz, J., González-Fernández, I., García-Gómez, H., Sánchez-Martín, L.,
889 Alonso, R., and Bermejo-Bermejo, V.: Current ozone levels threaten gross primary production and
890 yield of Mediterranean annual pastures and nitrogen modulates the response, *Atmospheric*
891 *Environment*, 95, 197-206, <http://dx.doi.org/10.1016/j.atmosenv.2014.05.073>, 2014.

892 Capriel, P.: Trends in organic carbon and nitrogen contents in agricultural soils in Bavaria (south
893 Germany) between 1986 and 2007, *European Journal of Soil Science*, 64, 445-454, 2013.

894 Cech, P. G., Pepin, S., and Korner, C.: Elevated CO₂ reduces sap flux in mature deciduous forest trees,
895 *Oecologia*, 137, 258-268, 2003.

896 Ceulemans, R., and Mousseau, M.: Effects of elevated atmospheric CO₂ on woody plants, *New*
897 *Phytologist*, 127, 1994.

898 Ciais, P., Wattenbach, M., Vuichard, N., Smith, P., Piao, S., Don, A., Luyssaert, S., Janssens, I.,
899 Bondeau, A., and Dechow, R.: The European carbon balance. Part 2: croplands, *Global Change*
900 *Biology*, 16, 1409-1428, 2010.

901 Ciais, P., Sabine, C., Bala, G., Bopp, L., Brovkin, V., Canadell, J., Chhabra, A., DeFries, R., Galloway, J.,
902 Heimann, M., Jones, C., Le Quéré, C., Myneni, R. B., Piao, S., and Thornton, P.: Carbon and Other
903 Biogeochemical Cycles. In: *Climate Change 2013: The Physical Science Basis. Contribution of Working*
904 *Group I to the Fifth Assessment Report of the Intergovernmental Panel on Climate Change* [Stocker,
905 T.F., D. Qin, G.-K. Plattner, M. Tignor, S.K. Allen, J. Boschung, A. Nauels, Y. Xia, V. Bex and P.M.
906 Midgley (eds.)]. Cambridge University Press, Cambridge, United Kingdom and New York, NY, USA.,
907 2013.

908 Clark, D. B., Mercado, L. M., Sitch, S., Jones, C. D., Gedney, N., Best, M. J., Pryor, M., Rooney, G. G.,
909 Essery, R. L. H., Blyth, E., Boucher, O., Harding, R. J., and Cox, P. M.: The Joint UK Land Environment
910 Simulator (JULES), Model description - Part 2: Carbon fluxes and vegetation, *Geoscientific Model*
911 *Development Discussions*, 4, 641-688, 10.5194/gmdd-4-641-2011, 2011.

912 CLRTAP: The UNECE Convention on Long-range Transboundary Air Pollution. Manual on
913 Methodologies and Criteria for Modelling and Mapping Critical Loads and Levels and Air Pollution
914 Effects, Risks and Trends: Chapter III Mapping Critical Levels for Vegetation, accessed via,
915 [http://icpvegetation.ceh.ac.uk/publications/documents/Chapter3-](http://icpvegetation.ceh.ac.uk/publications/documents/Chapter3-Mappingcriticallevelsforvegetation_000.pdf)
916 [Mappingcriticallevelsforvegetation_000.pdf](http://icpvegetation.ceh.ac.uk/publications/documents/Chapter3-Mappingcriticallevelsforvegetation_000.pdf), 2017.

917 Collins, W. J., Sitch, S., and Boucher, O.: How vegetation impacts affect climate metrics for ozone
918 precursors, *Journal of Geophysical Research: Atmospheres*, 115, D23308, 10.1029/2010JD014187,
919 2010.

920 Collins, W. J., Bellouin, N., Doutriaux-Boucher, M., Gedney, N., Halloran, P., Hinton, T., Hughes, J.,
921 Jones, C. D., Joshi, M., Liddicoat, S., Martin, G., O'Connor, F., Rae, J., Senior, C., Sitch, S., Totterdell, I.,
922 Wiltshire, A., and Woodward, S.: Development and evaluation of an Earth-System model –
923 HadGEM2, *Geosci. Model Dev.*, 4, 1051-1075, 10.5194/gmd-4-1051-2011, 2011.

924 Cooper, O. R., Parrish, D. D., Stohl, A., Trainer, M., Nedelec, P., Thouret, V., Cammas, J. P., Oltmans,
925 S. J., Johnson, B. J., Tarasick, D., Leblanc, T., McDermid, I. S., Jaffe, D., Gao, R., Stith, J., Ryerson, T.,
926 Aikin, K., Campos, T., Weinheimer, A., and Avery, M. A.: Increasing springtime ozone mixing ratios in
927 the free troposphere over western North America, *Nature*, 463, 344-348,
928 http://www.nature.com/nature/journal/v463/n7279/supinfo/nature08708_S1.html, 2010.

929 Cooper, O. R., Parrish, D., Ziemke, J., Balashov, N., Cupeiro, M., Galbally, I., Gilge, S., Horowitz, L.,
930 Jensen, N., and Lamarque, J.-F.: Global distribution and trends of tropospheric ozone: An
931 observation-based review, *Elementa: Science of the Anthropocene*, 2, 000029, 2014.

932 Cox, P. M., Betts, R. A., Jones, C. D., Spall, S. A., and Totterdell, I. J.: Acceleration of global warming
933 due to carbon-cycle feedbacks in a coupled climate model, *Nature*, 408, 184-187, 2000.

934 Cox, P. M.: Description of the TRIFFID dynamic global vegetation model, Hadley Centre technical
935 note 24, 2001.

936 Cruz, F. T., Pitman, A. J., and Wang, Y. P.: Can the stomatal response to higher atmospheric carbon
937 dioxide explain the unusual temperatures during the 2002 Murray-Darling Basin drought?, *Journal of*
938 *Geophysical Research: Atmospheres*, 115, 2010.

939 de Arellano, J. V.-G., van Heerwaarden, C. C., and Lelieveld, J.: Modelled suppression of boundary-
940 layer clouds by plants in a CO₂-rich atmosphere, *Nature geoscience*, 5, 701-704, 2012.

941 De Kauwe, M., Kala, J., Lin, Y.-S., Pitman, A., Medlyn, B., Duursma, R., Abramowitz, G., Wang, Y.-P.,
942 and Miralles, D.: A test of an optimal stomatal conductance scheme within the CABLE land surface
943 model, 8, 431-452, 2015.

944 Dentener, F., Stevenson, D., Ellingsen, K., van Noije, T., Schultz, M., Amann, M., Atherton, C., Bell, N.,
945 Bergmann, D., Bey, I., Bouwman, L., Butler, T., Cofala, J., Collins, B., Drevet, J., Doherty, R., Eickhout,
946 B., Eskes, H., Fiore, A., Gauss, M., Hauglustaine, D., Horowitz, L., Isaksen, I. S. A., Josse, B., Lawrence,
947 M., Krol, M., Lamarque, J. F., Montanaro, V., Müller, J. F., Peuch, V. H., Pitari, G., Pyle, J., Rast, S.,
948 Rodriguez, J., Sanderson, M., Savage, N. H., Shindell, D., Strahan, S., Szopa, S., Sudo, K., Van
949 Dingenen, R., Wild, O., and Zeng, G.: The Global Atmospheric Environment for the Next Generation,
950 *Environmental Science & Technology*, 40, 3586-3594, 10.1021/es0523845, 2006.

951 Derwent, R. G., Stevenson, D. S., Doherty, R. M., Collins, W. J., Sanderson, M. G., and Johnson, C. E.:
952 Radiative forcing from surface NO_x emissions: spatial and seasonal variations, *Climatic Change*, 88,
953 385-401, 10.1007/s10584-007-9383-8, 2008.

954 Ellsworth, D. S.: CO₂ enrichment in a maturing pine forest: are CO₂ exchange and water status in the
955 canopy affected?, *Plant, Cell and Environment*, 22, 461-472, 1999.

956 Emberson, L. D., Ashmore, M. R., Cambridge, H. M., Simpson, D., and Tuovinen, J.-P.: Modelling
957 stomatal ozone flux across Europe, *Environmental Pollution*, 109, 403-413, 2000.

958 Emberson, L. D., Simpson, D., Tuovinen, J.-P., Ashmore, M. R., and Cambridge, H. M.: Modelling and
959 mapping ozone deposition in Europe, *Water Air Soil Pollution*, 130, 577-582, 2001.

960 Engardt, M., Simpson, D., Schwikowski, M., and Granat, L.: Deposition of sulphur and nitrogen in
961 Europe 1900-2050. Model calculations and comparison to historical observations, *Tellus B: Chem.*
962 *Phys. Meteor.*, 69, 2017.

963 Etheridge, D. M., Steele, L. P., Langenfelds, R. L., Francey, R. J., M., B., and Morgan, V. I.: Natural and
964 anthropogenic changes in atmospheric CO₂ over the last 1000 years from air in Antarctic ice and firn,
965 *Journal of Geophysical Research*, 101(D2), 4115-4128, doi:10.1029/95JD03410, 1996.

966 Fagnano, M., Maggio, A., and Fumagalli, I.: Crops' responses to ozone in Mediterranean
967 environments, *Environmental Pollution*, 157, 1438-1444, 2009.

968 Fares, S., Vargas, R., Detto, M., Goldstein, A. H., Karlik, J., Paoletti, E., and Vitale, M.: Tropospheric
969 ozone reduces carbon assimilation in trees: estimates from analysis of continuous flux
970 measurements, *Global change biology*, 19, 2427-2443, 2013.

971 Felzer, B., Reilly, J., Melillo, J., Kicklighter, D., Sarofim, M., Wang, C., Prinn, R., and Zhuang, Q.: Future
972 Effects of Ozone on Carbon Sequestration and Climate Change Policy Using a Global Biogeochemical
973 Model, *Climatic Change*, 73, 345-373, 10.1007/s10584-005-6776-4, 2005.

974 Felzer, B. S. F., Kicklighter, D. W., Melillo, J. M., Wang, C., Zhuang, Q., and Prinn, R. G.: Ozone effects
975 on net primary productivity and carbon sequestration in the conterminous United States using a
976 biogeochemistry model, *Tellus*, 56B, 230-248, 2004.

977 Feng, Z., Kobayashi, K., and Ainsworth, E. A.: Impact of elevated ozone concentration on growth,
978 physiology, and yield of wheat (*Triticum aestivum* L.): a meta-analysis, *Global Change Biology*, 14,
979 2696-2708, 10.1111/j.1365-2486.2008.01673.x, 2008.

980 Fowler, D., Flechard, C., Cape, J. N., Storeton-West, R. L., and Coyle, M.: Measurements of Ozone
981 Deposition to Vegetation Quantifying the Flux, the Stomatal and Non-Stomatal Components, *Water,*
982 *Air, and Soil Pollution*, 130, 63-74, 10.1023/a:1012243317471, 2001.

983 Fowler, D., Pilegaard, K., Sutton, M., Ambus, P., Raivonen, M., Duyzer, J., Simpson, D., Fagerli, H.,
984 Fuzzi, S., and Schjørring, J. K.: Atmospheric composition change: ecosystems-atmosphere
985 interactions, *Atmospheric Environment*, 43, 5193-5267, 2009.

986 Franz, M., Simpson, D., Arneth, A., and Zaehle, S.: Development and evaluation of an ozone
987 deposition scheme for coupling to a terrestrial biosphere model, *Biogeosciences*, 14, 45-71,
988 doi:10.5194/bg-14-45-2017, 2017.

989 Friedlingstein, P., Cox, P., Betts, R., Bopp, L., von Bloh, W., Brovkin, V., Cadule, P., Doney, S., Eby, M.,
990 Fung, I., Bala, G., John, J., Jones, C., Joos, F., Kato, T., Kawamiya, M., Knorr, W., Lindsay, K.,
991 Matthews, H. D., Raddatz, T., Rayner, P., Reick, C., Roeckner, E., Schnitzler, K. G., Schnur, R.,
992 Strassmann, K., Weaver, A. J., Yoshikawa, C., and Zeng, N.: Climate-Carbon Cycle Feedback Analysis:
993 Results from the C4MIP Model Intercomparison, *Journal of Climate*, 19, 3337-3353,
994 10.1175/jcli3800.1, 2006.

995 Fuhrer, J., Val Martin, M., Mills, G., Heald, C. L., Harmens, H., Hayes, F., Sharps, K., Bender, J., and
996 Ashmore, M. R.: Current and future ozone risks to global terrestrial biodiversity and ecosystem
997 processes, *Ecology and Evolution*, 6, 8785-8799, 10.1002/ece3.2568, 2016.

998 Gedney, N., Cox, P. M., Bett, R. A., Boucher, O., Huntingford, C., and Stott, P. A.: Detection of a direct
999 carbon dioxide effect in continental river runoff records, *Nature*, 439, 835-838, 2006.

1000 Grantz, D., Gunn, S., and VU, H. B.: O₃ impacts on plant development: a meta-analysis of root/shoot
1001 allocation and growth, *Plant, cell & environment*, 29, 1193-1209, 2006.

1002 Harmens, H., Mills, G., Emberson, L. D., and Ashmore, M. R.: Implications of climate change for the
1003 stomatal flux of ozone: A case study for winter wheat, *Environmental Pollution*, 146, 763-770,
1004 <http://dx.doi.org/10.1016/j.envpol.2006.05.018>, 2007.

1005 Hayes, F., Wagg, S., Mills, G., Wilkinson, S., and Davies, W.: Ozone effects in a drier climate:
1006 implications for stomatal fluxes of reduced stomatal sensitivity to soil drying in a typical grassland
1007 species, *Global Change Biology*, 18, 948-959, 2012.

1008 Heikkinen, J., Ketoja, E., Nuutinen, V., and Regina, K.: Declining trend of carbon in Finnish cropland
1009 soils in 1974–2009, *Global Change Biology*, 19, 1456-1469, 10.1111/gcb.12137, 2013.

1010 Hofmockel, K. S., Zak, D. R., Moran, K. K., and Jastrow, J. D.: Changes in forest soil organic matter
1011 pools after a decade of elevated CO₂ and O₃, *Soil Biology and Biochemistry*, 43, 1518-1527,
1012 <http://dx.doi.org/10.1016/j.soilbio.2011.03.030>, 2011.

1013 Hoshika, Y., Watanabe, M., Inada, N., and Koike, T.: Ozone-induced stomatal sluggishness develops
1014 progressively in Siebold's beech (*Fagus crenata*), *Environmental Pollution*, 166, 152-156, 2012a.

1015 Hoshika, Y., Omasa, K., and Paoletti, E.: Whole-Tree Water Use Efficiency Is Decreased by Ambient
1016 Ozone and Not Affected by O₃-Induced Stomatal Sluggishness, *PLOS ONE*, 7, e39270,
1017 10.1371/journal.pone.0039270, 2012b.

1018 Hoshika, Y., Watanabe, M., Inada, N., and Koike, T.: Model-based analysis of avoidance of ozone
1019 stress by stomatal closure in Siebold's beech (*Fagus crenata*), *Annals of Botany*, 112, 1149-1158,
1020 2013.

1021 Hoshika, Y., Katata, G., Deushi, M., Watanabe, M., Koike, T., and Paoletti, E.: Ozone-induced stomatal
1022 sluggishness changes carbon and water balance of temperate deciduous forests., *Scientific Reports*,
1023 doi:10.1038/srep09871, 2015.

1024 Hurtt, G., Chini, L. P., Frolking, S., Betts, R., Feddema, J., Fischer, G., Fisk, J., Hibbard, K., Houghton,
1025 R., Janetos, A., and Jones, C. D.: Harmonization of land-use scenarios for the period 1500–2100: 600
1026 years of global gridded annual land-use transitions, wood harvest, and resulting secondary lands,
1027 *Climatic Change*, 109, 117-161, 2011.

1028 IPCC: Climate change 2013: The Physical Science Basis, IPCC Working Group I Contribution to AR5,
1029 2013.

1030 Jacobs, C. M. J.: Direct impact of atmospheric CO₂ enrichment on regional transpiration, Wageningen
1031 Agricultural University, 1994.

1032 Janssens, I. A., Freibauer, A., Ciais, P., Smith, P., Nabuurs, G.-J., Folberth, G., Schlamadinger, B.,
1033 Hutjes, R. W. A., Ceulemans, R., Schulze, E.-D., Valentini, R., and Dolman, A. J.: Europe's Terrestrial
1034 Biosphere Absorbs 7 to 12% of European Anthropogenic CO₂ Emissions, *Science*, 300, 1538-1542,
1035 10.1126/science.1083592, 2003.

1036 Jones, C. D., Cox, P., and Huntingford, C.: Uncertainty in climate–carbon-cycle projections associated
1037 with the sensitivity of soil respiration to temperature, *Tellus B*, 55, 642-648, 10.1034/j.1600-
1038 0889.2003.01440.x, 2003.

1039 Jung, M., Reichstein, M., Margolis, H. A., Cescatti, A., Richardson, A. D., Arain, M. A., Arneth, A.,
1040 Bernhofer, C., Bonal, D., Chen, J., Gianelle, D., Gobron, N., Kiely, G., Kutsch, W., Lasslop, G., Law, B.
1041 E., Lindroth, A., Merbold, L., Montagnani, L., Moors, E. J., Papale, D., Sottocornola, M., Vaccari, F.,
1042 and Williams, C.: Global patterns of land-atmosphere fluxes of carbon dioxide, latent heat, and
1043 sensible heat derived from eddy covariance, satellite, and meteorological observations, *Journal of*
1044 *Geophysical Research: Biogeosciences*, 116, n/a-n/a, 10.1029/2010JG001566, 2011.

1045 Kala, J., De Kauwe, M. G., Pitman, A. J., Medlyn, B. E., Wang, Y. P., Lorenz, R., and Perkins-Kirkpatrick,
1046 S. E.: Impact of the representation of stomatal conductance on model projections of heatwave
1047 intensity., *Scientific Reports*, 1-7, 10.1038/srep23418, 2016.

1048 Karlsson, P. E., Braun, S., Broadmeadow, M., Elvira, S., Emberson, L., Gimeno, B. S., Le Thiec, D.,
1049 Novak, K., Oksanen, E., Schaub, M., Uddling, J., and Wilkinson, M.: Risk assessments for forest trees:
1050 The performance of the ozone flux versus the AOT concepts, *Environmental Pollution*, 146, 608-616,
1051 <http://dx.doi.org/10.1016/j.envpol.2006.06.012>, 2007.

1052 Karnosky, D., Percy, K. E., Xiang, B., Callan, B., Noormets, A., Mankovska, B., Hopkin, A., Sober, J.,
1053 Jones, W., and Dickson, R.: Interacting elevated CO₂ and tropospheric O₃ predisposes aspen
1054 (*Populus tremuloides* Michx.) to infection by rust (*Melampsora medusae* f. sp. *tremuloidae*), *Global*
1055 *Change Biology*, 8, 329-338, 2002.

1056 Karnosky, D. F., Skelly, J. M., Percy, K. E., and Chappelka, A. H.: Perspectives regarding 50 years of
1057 research on effects of tropospheric ozone air pollution on US forests, *Environmental Pollution*, 147,
1058 489-506, 2007.

1059 Keeling, C. D., and Whorf, T. P.: Atmospheric CO₂ records from sites in the SIO air sampling network.
1060 In *Trends: A Compendium of Data on Global Change*, Carbon Dioxide Information Analysis Center,
1061 Oak Ridge National Laboratory, Oak Ridge, Tenn., U.S.A., 2004.

1062 Kitao, M., Löw, M., Heerdt, C., Grams, T. E., Häberle, K.-H., and Matyssek, R.: Effects of chronic
1063 elevated ozone exposure on gas exchange responses of adult beech trees (*Fagus sylvatica*) as related
1064 to the within-canopy light gradient, *Environmental Pollution*, 157, 537-544, 2009.

1065 Kjellström, E., Nikulin, G., Hansson, U., Strandberg, G., and Ullerstig, A.: 21st century changes in the
1066 European climate: uncertainties derived from an ensemble of regional climate model simulations,
1067 *Tellus A*, 63, 24-40, 2011.

1068 Kubiske, M., Quinn, V., Marquardt, P., and Karnosky, D.: Effects of Elevated Atmospheric CO₂ and/or
1069 O₃ on Intra- and Interspecific Competitive Ability of Aspen, *Plant biology*, 9, 342-355, 2007.

1070 Lamarque, J., Shindell, D. T., Josse, B., Young, P., Cionni, I., Eyring, V., Bergmann, D., Cameron-Smith,
1071 P., Collins, W. J., and Doherty, R.: The Atmospheric Chemistry and Climate Model Intercomparison
1072 Project (ACCMIP): overview and description of models, simulations and climate diagnostics,
1073 *Geoscientific Model Development*, 6, 179-206, 2013.

1074 Langner, J., Engardt, M., Baklanov, A., Christensen, J. H., Gauss, M., Geels, C., Hedegaard, G. B.,
1075 Nuterman, R., Simpson, D., and Soares, J.: A multi-model study of impacts of climate change on
1076 surface ozone in Europe, *Atmospheric Chemistry and Physics*, 12, 10423-10440, 2012a.

1077 Langner, J., Engardt, M., and Andersson, C.: European summer surface ozone 1990–2100,
1078 *Atmospheric Chemistry and Physics*, 12, 10097-10105, 2012b.

1079 Le Quéré, C., Moriarty, R., Andrew, R. M., Peters, G. P., Ciais, P., Friedlingstein, P., Jones, S. D., Sitch,
1080 S., Tans, P., Arneeth, A., Boden, T. A., Bopp, L., Bozec, Y., Canadell, J. G., Chini, L. P., Chevallier, F.,
1081 Cosca, C. E., Harris, I., Hoppema, M., Houghton, R. A., House, J. I., Jain, A. K., Johannessen, T., Kato,
1082 E., Keeling, R. F., Kitidis, V., Klein Goldewijk, K., Koven, C., Landa, C. S., Landschützer, P., Lenton, A.,
1083 Lima, I. D., Marland, G., Mathis, J. T., Metzl, N., Nojiri, Y., Olsen, A., Ono, T., Peng, S., Peters, W., Pfeil,
1084 B., Poulter, B., Raupach, M. R., Regnier, P., Rödenbeck, C., Saito, S., Salisbury, J. E., Schuster, U.,
1085 Schwinger, J., Séférian, R., Segschneider, J., Steinhoff, T., Stocker, B. D., Sutton, A. J., Takahashi, T.,
1086 Tilbrook, B., van der Werf, G. R., Viovy, N., Wang, Y. P., Wanninkhof, R., Wiltshire, A., and Zeng, N.:
1087 Global carbon budget 2014, *Earth Syst. Sci. Data*, 7, 47-85, 10.5194/essd-7-47-2015, 2015.

1088 Le Quéré, C., Andrew, R. M., Canadell, J. G., Sitch, S., Korsbakken, J. I., Peters, G. P., Manning, A. C.,
1089 Boden, T. A., Tans, P. P., Houghton, R. A., Keeling, R. F., Alin, S., Andrews, O. D., Anthoni, P., Barbero,
1090 L., Bopp, L., Chevallier, F., Chini, L. P., Ciais, P., Currie, K., Delire, C., Doney, S. C., Friedlingstein, P.,
1091 Gkritzalis, T., Harris, I., Hauck, J., Haverd, V., Hoppema, M., Klein Goldewijk, K., Jain, A. K., Kato, E.,
1092 Körtzinger, A., Landschützer, P., Lefèvre, N., Lenton, A., Lienert, S., Lombardozzi, D., Melton, J. R.,
1093 Metzl, N., Millero, F., Monteiro, P. M. S., Munro, D. R., Nabel, J. E. M. S., Nakaoka, S. I., O'Brien, K.,
1094 Olsen, A., Omar, A. M., Ono, T., Pierrot, D., Poulter, B., Rödenbeck, C., Salisbury, J., Schuster, U.,
1095 Schwinger, J., Séférian, R., Skjelvan, I., Stocker, B. D., Sutton, A. J., Takahashi, T., Tian, H., Tilbrook, B.,
1096 van der Laan-Luijkx, I. T., van der Werf, G. R., Viovy, N., Walker, A. P., Wiltshire, A. J., and Zaehle, S.:
1097 Global Carbon Budget 2016, *Earth Syst. Sci. Data*, 8, 605-649, 10.5194/essd-8-605-2016, 2016.

1098 Le Quéré, C., Andrew, R. M., Friedlingstein, P., Sitch, S., Pongratz, J., Manning, A. C., Korsbakken, J. I.,
1099 Peters, G. P., Canadell, J. G., Jackson, R. B., Boden, T. A., Tans, P. P., Andrews, O. D., Arora, V. K.,
1100 Bakker, D. C. E., Barbero, L., Becker, M., Betts, R. A., Bopp, L., Chevallier, F., Chini, L. P., Ciais, P.,
1101 Cosca, C. E., Cross, J., Currie, K., Gasser, T., Harris, I., Hauck, J., Haverd, V., Houghton, R. A., Hunt, C.
1102 W., Hurtt, G., Ilyina, T., Jain, A. K., Kato, E., Kautz, M., Keeling, R. F., Klein Goldewijk, K., Körtzinger,

1103 A., Landschützer, P., Lefèvre, N., Lenton, A., Lienert, S., Lima, I., Lombardozzi, D., Metzl, N., Millero,
1104 F., Monteiro, P. M. S., Munro, D. R., Nabel, J. E. M. S., Nakaoka, S.-I., Nojiri, Y., Padín, X. A., Peregón,
1105 A., Pfeil, B., Pierrot, D., Poulter, B., Rehder, G., Reimer, J., Rödenbeck, C., Schwinger, J., Séférian, R.,
1106 Skjelvan, I., Stocker, B. D., Tian, H., Tilbrook, B., van der Laan-Luijkx, I. T., van der Werf, G. R., van
1107 Heuven, S., Viovy, N., Vuichard, N., Walker, A. P., Watson, A. J., Wiltshire, A. J., Zaehle, S., and Zhu,
1108 D.: Global Carbon Budget 2017, *Earth Syst. Sci. Data Discuss*, in review, 2017.

1109 Leuzinger, S., and Körner, C.: Water savings in mature deciduous forest trees under elevated CO₂,
1110 *Global Change Biology*, 13, 2498-2508, doi:10.1111/j.1365-2486.2007.01467.x, 2007.

1111 Lin, Y.-S., Medlyn, B. E., Duursma, R. A., Prentice, I. C., Wang, H., Baig, S., Eamus, D., de Dios, V. R.,
1112 Mitchell, P., and Ellsworth, D. S.: Optimal stomatal behaviour around the world, *Nature Climate*
1113 *Change*, 5, 459-464, 2015.

1114 Lindroth, R. L.: Impacts of Elevated Atmospheric CO₂ and O₃ on Forests: Phytochemistry, Trophic
1115 Interactions, and Ecosystem Dynamics, *Journal of Chemical Ecology*, 36, 2-21, 10.1007/s10886-009-
1116 9731-4, 2010.

1117 Logan, J. A., Staehelin, J., Megretskaia, I. A., Cammas, J. P., Thouret, V., Claude, H., De Backer, H.,
1118 Steinbacher, M., Scheel, H. E., Stübi, R., Fröhlich, M., and Derwent, R.: Changes in ozone over
1119 Europe: Analysis of ozone measurements from sondes, regular aircraft (MOZAIC) and alpine surface
1120 sites, *Journal of Geophysical Research*, 117, 1-23, 2012.

1121 Lombardozzi, D., Levis, S., Bonan, G., Hess, P. G., and Sparks, J. P.: The Influence of Chronic Ozone
1122 Exposure on Global Carbon and Water Cycles, *Journal of Climate*, 28, 292-305, 10.1175/jcli-d-14-
1123 00223.1, 2015.

1124 Long, S. P., Ainsworth, E. A., Leakey, A. D. B., Nosberger, J., and Ort, D. R.: Food for Thought: Lower-
1125 Than-Expected Crop Yield Stimulation with Rising CO₂ Concentrations, *Science*, 312, 1918-1921,
1126 10.1126/science.1114722, 2006.

1127 Löw, M., Herbinger, K., Nunn, A., Häberle, K.-H., Leuchner, M., Heerdt, C., Werner, H., Wipfler, P.,
1128 Pretzsch, H., and Tausz, M.: Extraordinary drought of 2003 overrules ozone impact on adult beech
1129 trees (*Fagus sylvatica*), *Trees*, 20, 539-548, 2006.

1130 Loya, W. M., Pregitzer, K. S., Karberg, N. J., King, J. S., and Giardina, C. P.: Reduction of soil carbon
1131 formation by tropospheric ozone under increased carbon dioxide levels., *Nature*, 425, 705-707,
1132 2003.

1133 Luyssaert, S., Abril, G., Andres, R., Bastviken, D., Bellassen, V., Bergamaschi, P., Bousquet, P.,
1134 Chevallier, F., Ciais, P., Corazza, M., Dechow, R., Erb, K. H., Etiope, G., Fortems-Cheiney, A., Grassi, G.,
1135 Hartmann, J., Jung, M., Lathière, J., Lohila, A., Mayorga, E., Moosdorf, N., Njakou, D. S., Otto, J.,
1136 Papale, D., Peters, W., Peylin, P., Raymond, P., Rödenbeck, C., Saarnio, S., Schulze, E. D., Szopa, S.,
1137 Thompson, R., Verkerk, P. J., Vuichard, N., Wang, R., Wattenbach, M., and Zaehle, S.: The European
1138 land and inland water CO₂, CO, CH₄ and N₂O balance between 2001 and 2005, *Biogeosciences*, 9,
1139 3357-3380, 10.5194/bg-9-3357-2012, 2012.

1140 Massman, W. J.: A review of the molecular diffusivities of H₂O, CO₂, CH₄, CO, O₃, SO₂, NH₃, N₂O,
1141 NO, and NO₂ in air, O₂ and N₂ near STP, *Atmospheric Environment*, 32, 1111-1127,
1142 [http://dx.doi.org/10.1016/S1352-2310\(97\)00391-9](http://dx.doi.org/10.1016/S1352-2310(97)00391-9), 1998.

1143 Matyssek, R., Wieser, G., Ceulemans, R., Rennenberg, H., Pretzsch, H., Haberer, K., Löw, M., Nunn,
1144 A., Werner, H., and Wipfler, P.: Enhanced ozone strongly reduces carbon sink strength of adult beech
1145 (*Fagus sylvatica*)—Resume from the free-air fumigation study at Kranzberg Forest, *Environmental*
1146 *Pollution*, 158, 2527-2532, 2010a.

1147 Matyssek, R., Karnosky, D., Wieser, G., Percy, K., Oksanen, E., Grams, T., Kubiske, M., Hanke, D., and
1148 Pretzsch, H.: Advances in understanding ozone impact on forest trees: messages from novel
1149 phytotron and free-air fumigation studies, *Environmental Pollution*, 158, 1990-2006, 2010b.

1150 McLaughlin, S. B., Nosal, M., Wullschlegel, S. D., and Sun, G.: Interactive effects of ozone and climate
1151 on tree growth and water use in a southern Appalachian forest in the USA, *New Phytologist*, 174,
1152 109-124, 10.1111/j.1469-8137.2007.02018.x, 2007a.

1153 McLaughlin, S. B., Wullschleger, S. D., Sun, G., and Nosal, M.: Interactive effects of ozone and climate
1154 on water use, soil moisture content and streamflow in a southern Appalachian forest in the USA,
1155 *New Phytologist*, 174, 125-136, 10.1111/j.1469-8137.2007.01970.x, 2007b.

1156 Medlyn, B. E., Badeck, F. W., De Pury, D. G. G., Barton, C. V. M., Broadmeadow, M., Ceulemans, R.,
1157 De Angelis, P., Forstreuter, M., Jach, M. E., Kellomaki, S., Laitat, E., Marek, M., Philippot, S., Rey, A.,
1158 Strassemeier, J., Laitinen, K., Liozon, R., Portier, B., Roberntz, P., Wang, K., and Jstbid, P. G.: Effects
1159 of elevated [CO₂] on photosynthesis in European forest species: a meta-analysis of model
1160 parameters, *Plant, Cell & Environment*, 22, 1475-1495, doi:10.1046/j.1365-3040.1999.00523.x, 1999.

1161 Medlyn, B. E., Barton, C. V. M., Broadmeadow, M. S. J., Ceulemans, R., De Angelis, P., Forstreuter,
1162 M., Freeman, M., Jackson, S. B., Kellomaki, S., Laitat, E., Rey, A., Roberntz, P., Sigurdsson, B. D.,
1163 Strassemeier, J., Wang, K., Curtis, P. S., and Jarvis, P. G.: Stomatal conductance of forest species
1164 after long-term exposure to elevated CO₂ concentration: a synthesis, *New Phytologist*, 149, 247-264,
1165 2001.

1166 Medlyn, B. E., Duursma, R. A., Eamus, D., Ellsworth, D. S., Prentice, I. C., Barton, C. V., Crous, K. Y., de
1167 Angelis, P., Freeman, M., and Wingate, L.: Reconciling the optimal and empirical approaches to
1168 modelling stomatal conductance, *Global Change Biology*, 17, 2134-2144, 2011.

1169 Mercado, L. M., Bellouin, N., Sitch, S., Boucher, O., Huntingford, C., Wild, M., and Cox, P. M.: Impact
1170 of changes in diffuse radiation on the global land carbon sink, *Nature*, 458, 1014-1017,
1171 http://www.nature.com/nature/journal/v458/n7241/supinfo/nature07949_S1.html, 2009.

1172 Mills, G., Hayes, F., Wilkinson, S., and Davies, W. J.: Chronic exposure to increasing background
1173 ozone impairs stomatal functioning in grassland species, *Global Change Biology*, 15, 1522-1533,
1174 2009.

1175 Mills, G., Hayes, F., Simpson, D., Emberson, L., Norris, D., Harmens, H., and BÜKER, P.: Evidence of
1176 widespread effects of ozone on crops and (semi-)natural vegetation in Europe (1990–2006) in
1177 relation to AOT40- and flux-based risk maps, *Global Change Biology*, 17, 592-613, 10.1111/j.1365-
1178 2486.2010.02217.x, 2011b.

1179 Mills, G., Harmens, H., Wagg, S., Sharps, K., Hayes, F., Fowler, D., Sutton, M., and Davies, B.: Ozone
1180 impacts on vegetation in a nitrogen enriched and changing climate, *Environmental Pollution*, 208,
1181 898-908, 2016.

1182 Norby, R. J., Wullschleger, S. D., Gunderson, C. A., Johnson, D. W., and Ceulemans, R.: Tree responses
1183 to rising CO₂ in field experiments: implications for the future forest, *Plant, Cell and Environment*, 22,
1184 683-714, 1999.

1185 Norby, R. J., DeLucia, E. H., Gielen, B., Calfapietra, C., Giardina, C. P., King, J. S., Ledford, J., McCarthy,
1186 H. R., Moore, D. J. P., Ceulemans, R., De Angelis, P., Finzi, A. C., Karnosky, D. F., Kubiske, M. E., Lukac,
1187 M., Pregitzer, K. S., Scarascia-Mugnozza, G. E., Schlesinger, W. H., and Oren, R.: Forest response to
1188 elevated CO₂ is conserved across a broad range of productivity, *Proc. Natl. Acad. Sci. U. S. A.*, 102,
1189 18052-18056, 10.1073/pnas.0509478102, 2005.

1190 Nunn, A. J., Reiter, I. M., Häberle, K.-H., Langebartels, C., Bahnweg, G., Pretzsch, H., Sandermann, H.,
1191 and Matyssek, R.: Response patterns in adult forest trees to chronic ozone stress: identification of
1192 variations and consistencies, *Environmental Pollution*, 136, 365-369, 2005.

1193 Pacifico, F., Folberth, G. A., Jones, C. D., Harrison, S. P., and Collins, W. J.: Sensitivity of biogenic
1194 isoprene emissions to past, present, and future environmental conditions and implications for
1195 atmospheric chemistry, *Journal of Geophysical Research: Atmospheres*, 117, n/a-n/a,
1196 10.1029/2012JD018276, 2012.

1197 Paoletti, E., and Grulke, N. E.: Ozone exposure and stomatal sluggishness in different plant
1198 physiognomic classes, *Environmental Pollution*, 158, 2664-2671, 2010.

1199 Parrish, D. D., Law, K. S., Staehelin, J., Derwent, R., Cooper, O. R., Tanimoto, H., Volz-Thomas, A.,
1200 Gilge, S., Scheel, H. E., Steinbacher, M., and Chan, E.: Long-term changes in lower tropospheric
1201 baseline ozone concentrations at northern mid-latitudes, *Atmos. Chem. Phys.*, 12, 11485-11504,
1202 10.5194/acp-12-11485-2012, 2012.

1203 Percy, K. E., Awmack, C. S., Lindroth, R. L., Kubiske, M. E., Kopper, B. J., Isebrands, J., Pregitzer, K. S.,
1204 Hendrey, G. R., Dickson, R. E., and Zak, D. R.: Altered performance of forest pests under atmospheres
1205 enriched by CO₂ and O₃, *Nature*, 420, 403-407, 2002.

1206 Royal-Society: Ground-level ozone in the 21st century: future trends, impacts and policy
1207 implications, *Science Policy Report 15/08*, 2008.

1208 Samuelsson, P., Jones, C. G., Willén, U., Ullerstig, A., Gollvik, S., Hansson, U., Jansson, C., Kjellström,
1209 E., Nikulin, G., and Wyser, K.: The Rossby Centre Regional Climate model RCA3: model description
1210 and performance, *Tellus A*, 63, 4-23, 2011.

1211 Saxe, H., Ellsworth, D. S., and Heath, J.: Tree and forest functioning in an enriched CO₂ atmosphere,
1212 *New Phytologist*, 139, 395-436, doi:10.1046/j.1469-8137.1998.00221.x, 1998.

1213 Schulze, E.-D., Ciais, P., Luysaert, S., Schruppf, M., Janssens, I. A., Thiruchittampalam, B., Theloke, J.,
1214 Saurat, M., Bringezu, S., and Lelieveld, J.: The European carbon balance. Part 4: integration of carbon
1215 and other trace-gas fluxes, *Global Change Biology*, 16, 1451-1469, 2010.

1216 Schulze, E. D., Luysaert, S., Ciais, P., Freibauer, A., Janssens, I. A., and et al.: Importance of methane
1217 and nitrous oxide for Europe's terrestrial greenhouse-gas balance, *Nature Geosci*, 2, 842-850,
1218 http://www.nature.com/ngeo/journal/v2/n12/supinfo/ngeo686_S1.html, 2009.

1219 Sicard, P., De Marco, A., Troussier, F., Renoua, C., Vas, N., and Paoletti, E.: Decrease in surface ozone
1220 concentrations at Mediterranean remote sites and increase in the cities, *Atmospheric Environment*,
1221 79, 705-715, 2013.

1222 Simpson, D., Benedictow, A., Berge, H., Bergström, R., Emberson, L. D., Fagerli, H., Flechard, C. R.,
1223 Hayman, G. D., Gauss, M., and Jonson, J. E.: The EMEP MSC-W chemical transport model—technical
1224 description, *Atmospheric Chemistry and Physics*, 12, 7825-7865, 2012.

1225 Simpson, D., Andersson, C., Christensen, J. H., Engardt, M., Geels, C., Nyiri, A., Posch, M., Soares, J.,
1226 Sofiev, M., and Wind, P.: Impacts of climate and emission changes on nitrogen deposition in Europe:
1227 a multi-model study, *Atmospheric Chemistry and Physics*, 14, 6995-7017, 2014a.

1228 Simpson, D., Arneth, A., Mills, G., Solberg, S., and Uddling, J.: Ozone—the persistent menace:
1229 interactions with the N cycle and climate change, *Current Opinion in Environmental Sustainability*, 9,
1230 9-19, 2014b.

1231 Sitch, S., Cox, P. M., Collins, W. J., and Huntingford, C.: Indirect radiative forcing of climate change
1232 through ozone effects on the land-carbon sink, *Nature*, 448, 791-794,
1233 http://www.nature.com/nature/journal/v448/n7155/supinfo/nature06059_S1.html, 2007.

1234 Sitch, S., Friedlingstein, P., Gruber, N., Jones, S. D., Murray-Tortarolo, G., Ahlström, A., Doney, S. C.,
1235 Graven, H., Heinze, C., Huntingford, C., Levis, S., Levy, P. E., Lomas, M., Poulter, B., Viovy, N., Zaehle,
1236 S., Zeng, N., Arneth, A., Bonan, G., Bopp, L., Canadell, J. G., Chevallier, F., Ciais, P., Ellis, R., Gloor, M.,
1237 Peylin, P., Piao, S. L., Le Quéré, C., Smith, B., Zhu, Z., and Myneni, R.: Recent trends and drivers of
1238 regional sources and sinks of carbon dioxide, *Biogeosciences*, 12, 653-679, 10.5194/bg-12-653-2015,
1239 2015.

1240 Sleutel, S., De Neve, S., and Hofman, G.: Estimates of carbon stock changes in Belgian cropland., *Soil
1241 Use and Management*, 19, 166-171, 10.1079/SUM2003187, 2003.

1242 Sun, G. E., McLaughlin, S. B., Porter, J. H., Uddling, J., Mulholland, P. J., Adams, M. B., and Pederson,
1243 N.: Interactive influences of ozone and climate on streamflow of forested watersheds, *Global Change
1244 Biology*, 18, 3395-3409, 10.1111/j.1365-2486.2012.02787.x, 2012.

1245 Tai, P. K. A., Val Martin, M., and Heald, C. L.: Threat to future global food security from climate
1246 change and ozone air pollution, *Nature Climate Change*, 4, 817 - 821, 2014.

1247 Talhelm, A. F., Pregitzer, K. S., Kubiske, M. E., Zak, D. R., Company, C. E., Burton, A. J., Dickson, R. E.,
1248 Hendrey, G. R., Isebrands, J. G., Lewin, K. F., Nagy, J., and Karnosky, D. F.: Elevated carbon dioxide
1249 and ozone alter productivity and ecosystem carbon content in northern temperate forests, *Global
1250 Change Biology*, 20, 2492-2504, 10.1111/gcb.12564, 2014.

1251 Tricker, P. J., Pecchiari, M., Bunn, S. M., Vaccari, F. P., Peressotti, A., Miglietta, F., and Taylor, G.:
1252 Water use of a bioenergy plantation increases in a future high CO₂ world, *Biomass and Bioenergy*,
1253 33, 200-208, 2009.

1254 Tuovinen, J.-P., Emberson, L., and Simpson, D.: Modelling ozone fluxes to forests for risk assessment:
1255 status and prospects, *Annals of Forest Science*, 66, 1-14, 2009.

1256 Tuovinen, J., Hakola, H., Karlsson, P., and Simpson, D.: Air pollution risks to Northern European
1257 forests in a changing climate, *Climate Change, Air Pollution and Global Challenges Understanding*
1258 *and Perspectives from Forest Research*, 2013.

1259 Uddling, J., Teclaw, R. M., Pregitzer, K. S., and Ellsworth, D. S.: Leaf and canopy conductance in aspen
1260 and aspen-birch forests under free-air enrichment of carbon dioxide and ozone, *Tree Physiology*, 29,
1261 1367-1380, 2009.

1262 Verstraeten, W. W., Neu, J. L., Williams, J. E., Bowman, K. W., Worden, J. R., and Boersma, K. F.:
1263 Rapid increases in tropospheric ozone production and export from China, *Nature Geoscience* 8, 690-
1264 695, 2015.

1265 Vingarzan, R.: A review of surface ozone background levels and trends, *Atmospheric Environment*,
1266 38, 3431-3442, <https://doi.org/10.1016/j.atmosenv.2004.03.030>, 2004.

1267 Weedon, G. P., Gomes, S., Viterbo, P., Österle, H., Adam, J. C., Bellouin, N., Boucher, O., and Best, M.
1268 J.: The WATCH Forcing Data 1958-2001: a meteorological forcing dataset for land surface- and
1269 hydrological models. , WATCH Tech. Rep. 22, 41p (available at www.eu-watch.org/publications).
1270 2010.

1271 Weedon, G. P., Gomes, S., Viterbo, P., Shuttleworth, W. J., Blyth, E., Österle, H., Adam, J. C., Bellouin,
1272 N., Boucher, O., and Best, M.: Creation of the WATCH Forcing data and its use to assess global and
1273 regional reference crop evaporation over land during the twentieth century, *Journal of*
1274 *Hydrometeorology*, 12, 823-848, doi: 10.1175/2011JHM1369.1., 2011.

1275 Wilkinson, S., and Davies, W. J.: Ozone suppresses soil drying-and abscisic acid (ABA)-induced
1276 stomatal closure via an ethylene-dependent mechanism, *Plant, Cell & Environment*, 32, 949-959,
1277 2009.

1278 Wilkinson, S., and Davies, W. J.: Drought, ozone, ABA and ethylene: new insights from cell to plant to
1279 community, *Plant, Cell & Environment*, 33, 510-525, 10.1111/j.1365-3040.2009.02052.x, 2010.

1280 Wittig, V. E., Ainsworth, E. A., and Long, S. P.: To what extent do current and projected increases in
1281 surface ozone affect photosynthesis and stomatal conductance of trees? A meta-analytic review of
1282 the last 3 decades of experiments, *Plant, Cell & Environment*, 30, 1150-1162, 10.1111/j.1365-
1283 3040.2007.01717.x, 2007.

1284 Wittig, V. E., Ainsworth, E. A., Naidu, S. L., Karnosky, D. F., and Long, S. P.: Quantifying the impact of
1285 current and future tropospheric ozone on tree biomass, growth, physiology and biochemistry: a
1286 quantitative meta-analysis, *Global Change Biology*, 15, 396-424, 10.1111/j.1365-2486.2008.01774.x,
1287 2009.

1288 Wullschleger, S. D., Gunderson, C. A., Hanson, P. J., Wilson, K. B., and Norby, R. J.: Sensitivity of
1289 stomatal and canopy conductance to elevated CO₂ concentration; interacting variables and
1290 perspectives of scale, *New Phytologist*, 153, 485-496, doi:10.1046/j.0028-646X.2001.00333.x, 2002.

1291 Young, P., Arneth, A., Schurgers, G., Zeng, G., and Pyle, J. A.: The CO₂ inhibition of terrestrial isoprene
1292 emission significantly affects future ozone projections, *Atmospheric Chemistry and Physics*, 9, 2793-
1293 2803, 2009.

1294 Young, P., Archibald, A., Bowman, K., Lamarque, J.-F., Naik, V., Stevenson, D., Tilmes, S., Voulgarakis,
1295 A., Wild, O., and Bergmann, D.: Pre-industrial to end 21st century projections of tropospheric ozone
1296 from the Atmospheric Chemistry and Climate Model Intercomparison Project (ACCMIP),
1297 *Atmospheric Chemistry and Physics*, 13, 2063-2090, 2013.

1298 Zaehle, S.: Terrestrial nitrogen-carbon cycle interactions at the global scale, *Philosophical*
1299 *Transactions of the Royal Society B: Biological Sciences*, 368, 20130125, 10.1098/rstb.2013.0125,
1300 2013.

1301 Zak, D. R., Pregitzer, K. S., Kubiske, M. E., and Burton, A. J.: Forest productivity under elevated CO₂
1302 and O₃: positive feedbacks to soil N cycling sustain decade-long net primary productivity
1303 enhancement by CO₂, *Ecology Letters*, 14, 1220-1226, 10.1111/j.1461-0248.2011.01692.x, 2011.

1304

1305

1306

1307

1308

1309

1310

1317